THE DEVELOPMENT OF A DIELECTRIC SEPARATION TECHNIQUE FOR DIAMOND

by

Marek Adam Wiacek

Thesis submitted for The Degree of Master of Philosophy

Department of Mineral Technology
Imperial College of Science and Technology
London
SW7 2BP

ABSTRACT

Despite its apparent potential the separation of minerals according to their dielectric constants has yet to be developed as an industrial process. This thesis discusses the development of dielectric separation of diamonds from the minerals in Kimberlite.

The introduction summarises the state of the art of dielectric separation since its development in the 1920's up to present day, together with its possible application and suitability for the recovery of diamonds.

The practical work was divided into two sections:

(1) the use of matrix elements polarised in uniform and non-uniform fields

(11) the use of an isodynamic field to achieve reciprocal displacement of diamond and kimberlite particles.

With the matrix systems the separation depends on kimberlite attraction and diamond repulsion. The tests in both field configurations showed that whilst it was possible to attract and retain particles, the repulsion effect was hindered by mechanical trapping of particles.

Tests with the isodynamic field were carried out in horizontal and vertical modes of operation. The horizontal mode was shown to be more efficient, giving 100 % diamond recovery and the best results in terms of diamond grade. The development of a double isodynamic profile is discussed which could further improve separation performance and efficiency.

ACKNOWLEDGEMENTS

I would like to offer my sincere thanks to the following members of the Department of Mineral Resources Engineering: Dr U. Ts. Andres, Senior Research Fellow, with whom I have worked for two years; Professor H E Cohen, Head of the Mineral Technology Section, my supervisor, for help and guidance; the departmental staff, both academic and technical, who contributed help and advice; and to Miss S Curley for typing.

CONTENTS

LIST OF TABLES

LIST OF FIGURES

LIST OF PLATES

Chapter 1. INTRODUCTION

The work described in this thesis was carried out as part of a research project on "Electrical methods of diamond liberation and separation" and was sponsored by De Beers Diamond Corporation. One of its objectives was to study the use of differences in dielectric properties for the separation of diamond from other minerals in the kimberlite.

1.1. Historical development of dielectric separation

Electrodynamic techniques of moving small charged particles in an electrical field have been known for some time, the main application being in electrostatic separation. The Inverse square law developed by Coulomb in the late 18th Century describes the dynamic interactions of electrically charged particles in both vacuum and dielectric media. However, the study of dielectric properties as a means of mineral separation began only in the early 1920's. A process was developed by H. S. Hatfield (1) at the Royal School of Mines. The separation depends on the action of a non uniform electrostatic field upon uncharged but polarised particles and is analogous to magnetic separation in some respects. Despite this analogy and the use of similarly structured mathematical expressions for the forces involved in both magnetic and dielectric separation, it is impossible to carry out dielectric separations in air for two reasons. Firstly, air has a lower dielectric constant than any mineral, therefore all mineral particles would

be deflected in the same direction under the influence of the electrostatic field and selective spatial displacement of minerals is not possible. Secondly, due to the low ionization threshold of air the electrical fields would have to be of very low intensity, so the resultant force on a mineral particle would also be very small. It is necessary to use a dielectric liquid which must be an insulator in order to maintain a large electrical field without the passage of a large current.

The Hatfield process utilised a liquid dielectric polarised in a non-uniform electric field for separating mineral particles. This non-uniformity produces a difference in charge on opposite sides of the particles, which causes particles to move up or down the field gradient. Particles with higher dielectric constants than the liquid will move up the gradient, those with a lower dielectric constant will move down the gradient.

Hatfield's separation process was based on the selective deposition of particles with a dielectric constant greater than the liquid medium on sharp electrode edges at which the potential gradient is greatest. The particles of dielectric constant lower than the liquid moved away from the electrodes and were discharged from the separator (Figure 1.1). The apparatus is basically a chamber made from insulating material with a series of zig-zag shaped pieces of metal mounted inside which act as electrodes for the precipitation

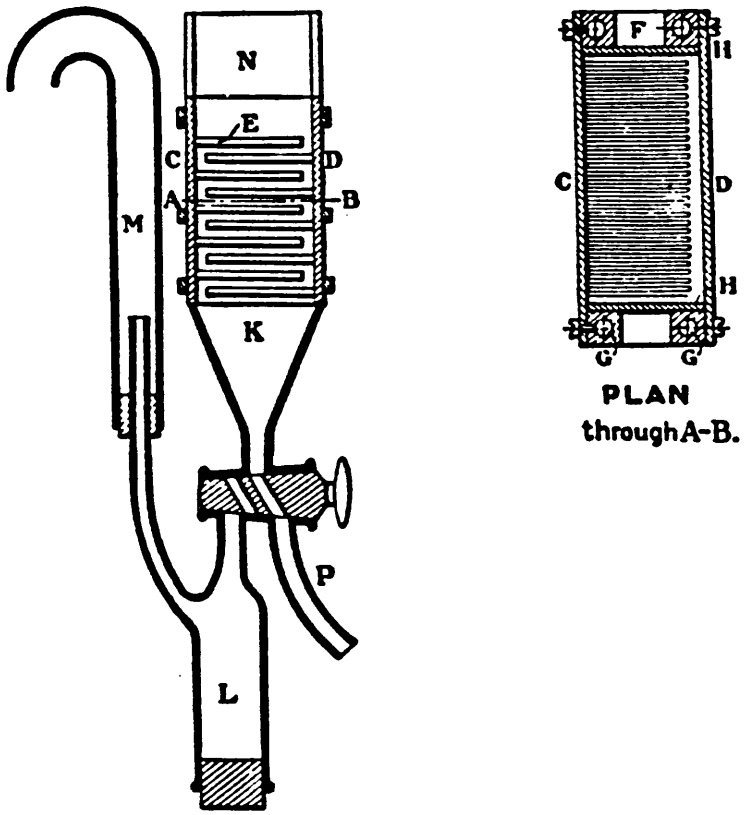

Figure 1.1. Laboratory Dielectric Separator (After Hatfield)(1)

of particles of higher dielectric constant than the liquid.

Hatfield used a mixture of nitrobenzene (dielectric constant 36) and kerosene (dielectric constant 2) as liquid dielectric medium. Appropriate proportions could be used to provide a variety of dielectric constants between 36 and 2 for treating a wide range of mineral mixtures.

Hatfield's process was originally tested on a Cornish tin ore to separate 1 % of cassiterite ($\varepsilon p > 81$) from quartz ($\varepsilon p \simeq 4.5$). Subsequently a plant for the treatment of sandstone from Colorado was built for a throughput of 1 ton per day.

Hatfield introduced to mineral processing a previously unused physical parameter, the possibility of treating ores not amenable to other methods. However, the Hatfield process was small scale and intermittent, requiring cyclic stopage for the removal of one or both products and was limited to minerals having significantly higher dielectric constants than the liquid medium. It employed relatively weak fields generated by voltages in the range of 100 to 400V, 200V being usual. With higher voltages Hatfield might have been able to treat mineral mixtures with much closer dielectric constants.

The liquid dielectric medium used was hazardous to use being poisonous and inflamable; this was probably the most serious obstacle to the adoption of dielectric separation on a larger industrial scale or as an analytical laboratory method.

Since the 1920's dielectric separation has branched into two technological directions, dielectric precipitation of solid impurities from liquids and gases without any selective separation of solids and dielectric separation of mineral mixtures as per Hatfields patent (2). The process of dielectric precipitation has been applied on an industrial scale in the oil and petrochemical fields, for the removal of solid and liquid impurities from liquid dielectrics such as oil and fuels, as well as for the purification of organic liquids in general.

Dielectric separation of mineral mixtures has remained on a small batch scale, for mineralogical analysis, or as a prototype process. Even the most recent publications still follow the original ideas outlined by Hatfield. For example a separator developed fairly recently by the U.S. Bureau of Mines (3) uses a live rotating drum electrode covered with a series of parallel wires. This drum is half immersed in a dielectric fluid, a second screen electrode being completely immersed. The method of separation by selective attraction and repulsion of particles is shown in Figure 1.2. The process was initially tested

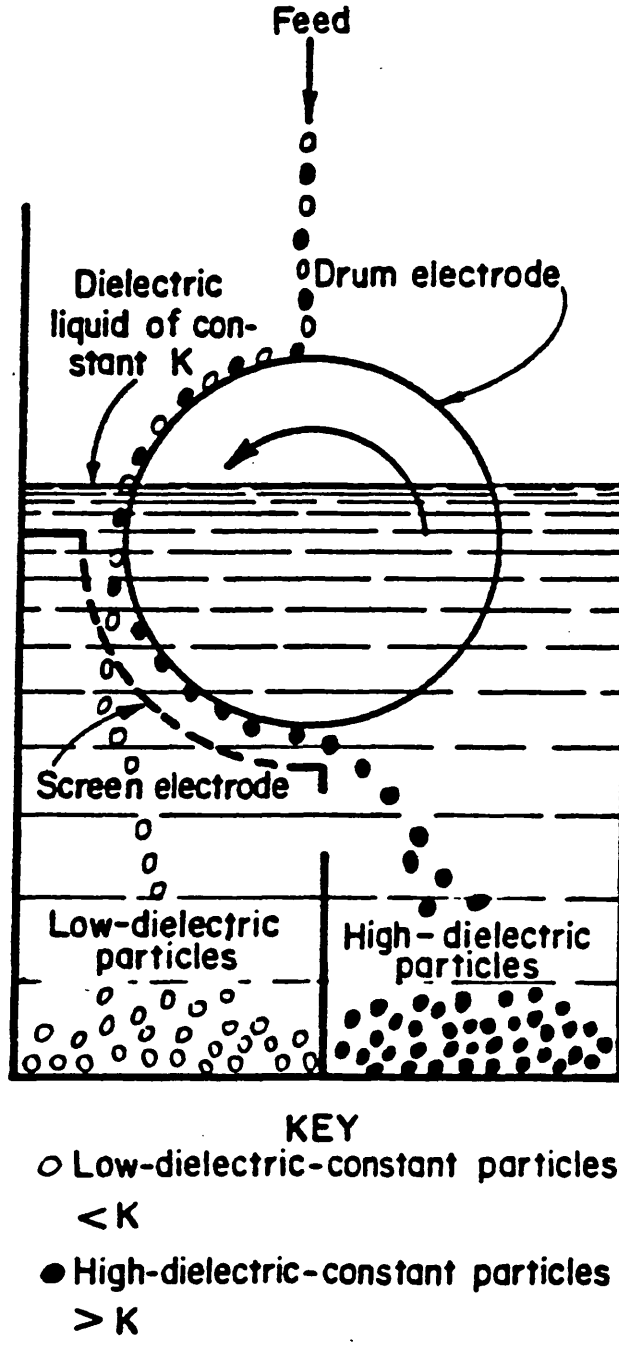

Figure 1.2. U.S. Bureau of Mines Dielectric Separator

on a mixture of 90 % quartz ($\varepsilon p \simeq 4.5$) and 10 % rutile ($\varepsilon p > 81$). The applied voltage was 1000V, giving a field strength between electrodes of 3×10^4 Vm^{-1}. The dielectrics used were mixtures of nitrobenzene-kerosene, ethanol-xylene and propanol-xylene.

1.2. Dielectric separation for diamond recovery.

The respective dielectric constants of diamond and of the other minerals in kimberlite make dielectric separation seemingly an ideal process for diamond separation as diamond has a lower dielectric constant ($\varepsilon p = 5.7$) than all kimberlite minerals ($\varepsilon p > 7.4$), except quartz ($\varepsilon p = 4.5$). These low and relatively close values of dielectric constants necessitate several changes from the separation process employed by Hatfield (1). The process will have to employ a high voltage in order to produce the field strengths of several hundred kilovolts per metre needed to achieve adequate separation. A liquid medium of intermediate relative permittivity needs to be used and, fortunately for this project, a petroleum by-product of suitable permittivity and breakdown threshold has been found: Di-n-butyl phthalate. This liquid has a dielectric constant of 6.1, is clear, colourless, cheap, relatively stable as well as non explosive.

For diamond recovery, the use of high voltage has the added attraction of providing some security against pilfering.

Chapter 2. INITIAL DIELECTRIC SEPARATION TESTS

The work can be divided into two main sections depending on the type of separation technique employed. The initial tests with matrix elements polarised in uniform and non uniform fields used the repulsion and attraction of particles, depending on their dielectric constants relative to that of the dielectric liquid medium. In later tests an isodynamic non-uniform field where the force on a particle is constant over the whole field was used for the reciprocal spatial displacement of particles in a direction governed by the relative value of the dielectric constant of the particle to that of the dielectric medium.

With a matrix, separation results from the attraction/repulsion forces between matrix elements and the particles to be separated. The matrix elements, being 2 to 3 times larger than the particles to be separated, become polarised under the influence of a uniform or non-uniform external field. The polarised matrix elements produce internal fields which attract or repel neighbouring particles, thus causing the separation effect.

2.1. Separation tests using matrix elements in an external uniform polarising field

2.1.1. Introduction

The initial model used for dielectric separation was that of matrix elements in an external, polarising,

magnetic field for separating diamagnetic and paramagnetic minerals.

The use of matrix elements for separation in an external, polarising, magnetic field is well known, Andres (4) has developed equations which describe the attraction/repulsion zones on matrix elements due to the influence of an external magnetic field.

The magnetic model provided the idea for using a dielectric instead of a magnetic medium to investigate whether such a system could be used, for example, to separate diamond/kimberlite mixtures. In a liquid dielectric the particles of lower dielectric constant (diamond) should pass through the system whilst particles of higher dielectric constant (kimberlite) should be retained by the matrix medium.

For the dielectric medium the equations of electrical force were first developed by Andres (5) and can be used to define the attraction/repulsion zones which arise on particles and also the magnitudes of the forces involved, not only those which arise between particles and matrix elements but also those which arise between individual particles leading to the formation of particle chains and clusters.

2.1.2. Development of equations of dipole-dipole interaction in a liquid dielectric medium.

Consider a sphere in an external polishing field,

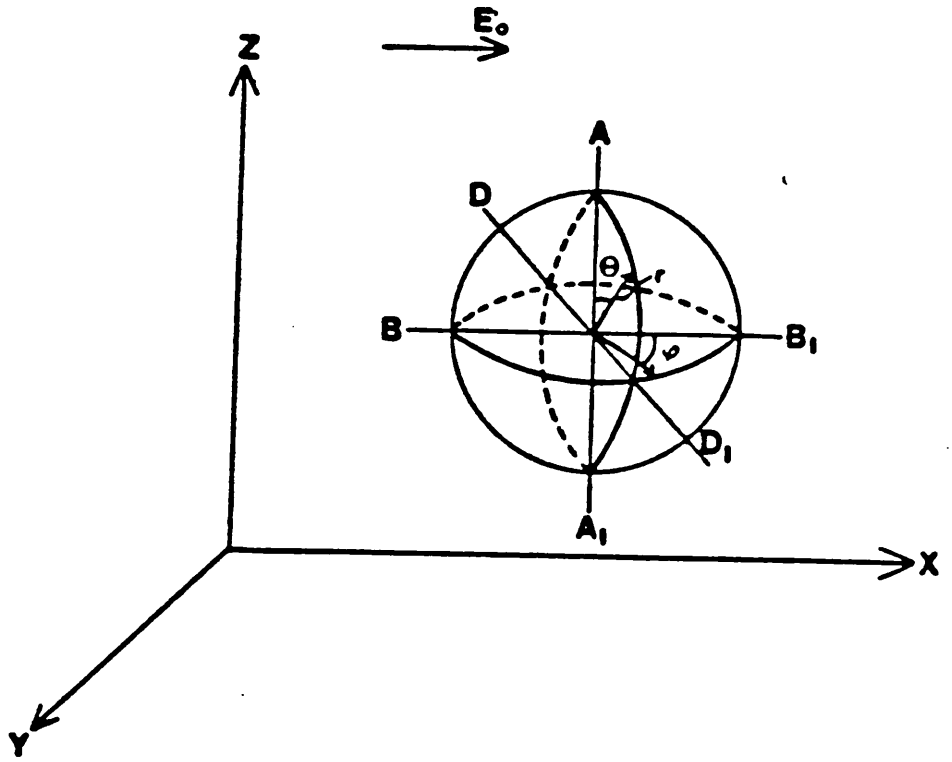

Figure 2.1.1. The Chosen System of Spherical Co-ordinates

(Figure 2.1.1.). Three force components need to be considered, Fr in a radial direction, and F_θ and F_ϕ the tangential components in the longitudinal and latitudinal directions respectively.

The external potential ϕ_e for a spherical particle in an electrical field E_o is

$$\phi_e = -\bar{E}_o\bar{r} + A\bar{E}_o \frac{\bar{r}}{r^3} \quad (1)$$

The internal field of a sphere is

$$E_i = E_o\left(1 - \frac{A}{R^3}\right) \quad (2)$$

The parameter A for a sphere can be found from the solution for its polarisation in a uniform electrical field. Therefore

$$A = R^3 \, 4\pi\xi_o \frac{(\varepsilon_p - \varepsilon_l)}{(\varepsilon_p + 2\varepsilon_l)} \quad (3)$$

Here R is the radius of the sphere, ε_l and ε_p dielectric constants of liquid and sphere respectively.
The external field in the vicinity of the sphere is

$$\bar{E}_e = -\operatorname{grad}\phi_e \quad (4)$$

In the spherical co-ordinate system

$$X = r \sin\theta \cos\phi \quad (5)$$

From equations (1) and (5), the external potential is

$$\phi_e = -E_o \, r \sin\theta \cos\phi \left[1 - \frac{A}{r^3}\right] \quad (6)$$

So the external field is

$$\bar{E}_e = -\text{grad}\,\phi_e = E_r\bar{i}_r + E_\theta\bar{i}_\theta + E_\phi\bar{i}_\phi \tag{7}$$

and also

$$\bar{E}_e^2 = E_r^2 + E_\theta^2 + E_\phi^2 \tag{8}$$

From the expression for the gradient of the field in spherical co-ordinates:

$$\left.\begin{aligned} E_r^2 &= \left|\frac{\partial\phi}{\partial r}e\right|^2 = E_o^2 \sin^2\theta \cos^2\phi \,(1 + \frac{2A}{r^3})^2 \\ E^2 &= \left|\frac{1}{r}\frac{\partial\phi_e}{\partial\theta}\right|^2 = E_o^2 \cos^2\theta \cos^2\phi \,(1 - \frac{A}{r^3})^2 \\ E^2 &= \left|\frac{1}{r\sin\theta}\frac{\partial\phi_e}{\partial\theta}\right|^2 = E_o^2 \sin^2 \,(1 - \frac{A}{r^3})^2 \end{aligned}\right\} \tag{9}$$

Substitution of equation (9) into equation (8) gives

$$E_e^2 = E_o^2\left[\sin^2\theta\cos^2\phi\,(1 + \frac{2A}{r^3})^2 + \cos^2\theta\cos^2\phi(1 - \frac{A}{r^3})^2 + \right.$$
$$\left. + \sin^2\phi\,(1 - \frac{A}{r^3})^2\right] \tag{10}$$

The dipole-dipole interaction is the force acting on a particle of radius a in the external field of spherical particles of radius R.

$$\bar{F} = B\ \text{grad}\ (E_e)^2 \tag{11}$$

where

$$B = 4\pi\xi_o \frac{\xi_\iota a^3}{2} \frac{(\varepsilon_p - \varepsilon_\iota)}{(\varepsilon_p + 2\varepsilon_\iota)} \tag{12}$$

So the radial component of the force

$$Fr = B\frac{dE_e^2}{dr} = B\,E_o^2\Big[2\sin^2\theta\cos^2\phi\,(1+\frac{2A}{r^3})(-\frac{6A}{r^4}) +$$

$$+ 2\cos^2\theta\cos^2\phi\,(1-\frac{A}{r^3})(\frac{3A}{r^4}) + 2\sin^2\phi\,(1-\frac{A}{r^3})(\frac{3A}{r^4})\Big] =$$

$$= \frac{BE_o^2 6A}{r^4}\Big[-2\sin^2\theta\cos^2\phi\,(1+\frac{2A}{r^3}) + \cos^2\theta\cos^2\phi$$

$$(1-\frac{A}{r^3}) + \sin^2\phi\,(1-\frac{A}{r^3})\Big] = \qquad (13)$$

$$= \frac{6BE_o^2A}{r^4}\Big[-3\sin^2\theta\cos^2\phi + 1 - \frac{A}{r^3}\big[3\sin^2\theta\cos^2\phi + 1\big]\Big] \qquad (14)$$

Then substituting for B and A introducing m the dielectric constant of the matrix element:

$$F = \frac{1}{R}\,\frac{3\varepsilon_l 4\pi\varepsilon_o a^3(\varepsilon_p-\varepsilon_l)}{(\varepsilon_p+2\varepsilon_l)}\;E_o^2\;\frac{4\pi\varepsilon_o(\varepsilon_m-\varepsilon_l)}{(\varepsilon_m+2\varepsilon_l)}$$

$$\Big[1 - 3\sin^2\theta\cos^2\phi - \frac{4\pi\varepsilon_o(\varepsilon_m-\varepsilon_l)}{(\varepsilon_m+2\varepsilon_l)}\cdot$$

$$(3\sin^2\theta\cos^2\phi + 1)\Big] \qquad (15)$$

$$= \frac{1}{R}\,\frac{3\varepsilon_l 4\pi\varepsilon_o a^3(\varepsilon_p-\varepsilon_l)(\varepsilon_m-\varepsilon_l)}{(\varepsilon_p+2\varepsilon_l)(\varepsilon_m+2\varepsilon_l)}\cdot E_o^2\cdot$$

$$\Big[\frac{3\varepsilon_l 4\pi\varepsilon_o}{2(\varepsilon_l+\varepsilon_m)} - 3\sin^2\theta\cos^2\phi\,\frac{4\pi\varepsilon_o(2\varepsilon_m+\varepsilon_l)}{(2\varepsilon_l+\varepsilon_m)}\Big] \qquad (16)$$

Rearranging:

$$F = \frac{1}{R} \frac{9(\varepsilon_l)^2 \, 4\pi\varepsilon_o \, a^3(\varepsilon_p - \varepsilon_l)\,(\varepsilon_m - \varepsilon_l)}{(\varepsilon_p + 2\varepsilon_l)(\varepsilon_m + 2\varepsilon_l)^2} \cdot E_o^2 \cdot$$

$$\left[1 - \sin^2\theta \cos^2\phi \left[1 + 2\frac{\varepsilon_m}{\varepsilon_l}\right]\right] \qquad (17)$$

Thus for a particular matrix element and a particular sphere

$$\frac{1}{R} \frac{9(\varepsilon_l)^2 \, 4\pi\varepsilon_o a^3(\varepsilon_p - \varepsilon_l)(\varepsilon_m - \varepsilon_l)\,[E_o]^2}{(\varepsilon_p + 2\varepsilon_l)(\varepsilon_m + 2\varepsilon_l)^2}$$

will be a constant α

Therefore

$$Fr = \alpha\left(1 - \sin^2\theta \cos^2\phi \,(1 + 2\frac{\varepsilon_m}{\varepsilon_l})\right)$$

such that at A, A_1, (Figure 2.1.3) where $\theta = 0$ or π and when $\phi = \pi/2$ or $3\pi/2$

$$Fr = \alpha$$

i.e. all along the equator the force has a constant value α.

At a point on the pole where $\theta = \pi/2$ and $\phi = 0, \pi$

$$Fr = -2\alpha\frac{\varepsilon_m}{\varepsilon_l}$$

When Fr is positive there is attraction between particles and when Fr is negative repulsion occurs.

From the differentiation of equations (9) for the squared fields E_θ^2 and E_ϕ^2 the expression for the

tangential component of the force in the longitudinal direction is

$$F_\theta = \frac{B}{r} E_o^2 \left[2 \sin\theta \cos\theta \cos^2\phi \left(1 + \frac{2A}{r^3}\right)^2 \right.$$

$$\left. -2\sin\theta \cos\theta \cos^2\phi \left(1 - \frac{A}{r^3}\right)^2 \right] = \frac{B}{r} E_o^2 .$$

$$\left[2\sin\theta \cos\theta \cos^2\phi \left[\left(1 + \frac{2A}{r^3}\right)^2 - \left(1 - \frac{A}{r^3}\right)^2\right]\right] \quad (18)$$

The tangential component in the latitudinal direction is

$$F_\phi = \frac{B}{r\sin\theta} E_o^2 \left[-2\sin^2\theta \sin\phi \cos\phi \left(1 + \frac{2A}{r^3}\right)^2 \right.$$

$$\left. -2\cos^2\theta \sin\phi \cos\phi \left(1 - \frac{A}{r^3}\right)^2 + 2\sin\phi \cos\phi \left(1 - \frac{A}{r^3}\right)^2 \right] \quad (19)$$

The radial component of the force gives rise to the attraction/repulsion forces between particles. The tangential components cause particles to revolve around each other until they achieve an equilibrium position.

2.1.3. Experimental

The separation system was arranged so that the attraction zones for the higher dielectric kimberlite minerals were parallel to the liquid flow, whilst the zones of attraction for the lower dielectric diamonds were normal to the direction of liquid flow. Thus diamond particles, being more strongly affected by the liquid flow, should be dislodged from the matrix elements and would be washed through the system, whilst

kimberlite particles should be retained by the matrix elements despite the flow of liquid.

Initial tests were carried out to investigate whether kimberlite particles could be retained. The apparatus is shown in Figure 2.1.2. Di-n-butyl phthalate was used as the dielectric liquid. Steel and glass balls of diameter 12 mm were tested as matrix media, to investigate the effects of using media with different relative permittivities (Steel $\xi_R = \infty$ being a conductor and Glass $\xi_R \simeq 4.1$). The polythene insulating rings B prevented contact between the matrix elements and the top and bottom gauzes. In the case of steel balls this prevented a current flow between the electrodes.

2.1.4. Test Procedure

a) With the field switched on, the test material was allowed to flow through the separator and repelled material was collected in the tube above the lower tap, the upper tap being open.

b) After completion of the separation process the field remained switched on and the upper tap was closed.

c) The field was then switched off and the repelled material was discharged by opening the lower tap. The attracted material retained in the matrix was then washed out of the separator.

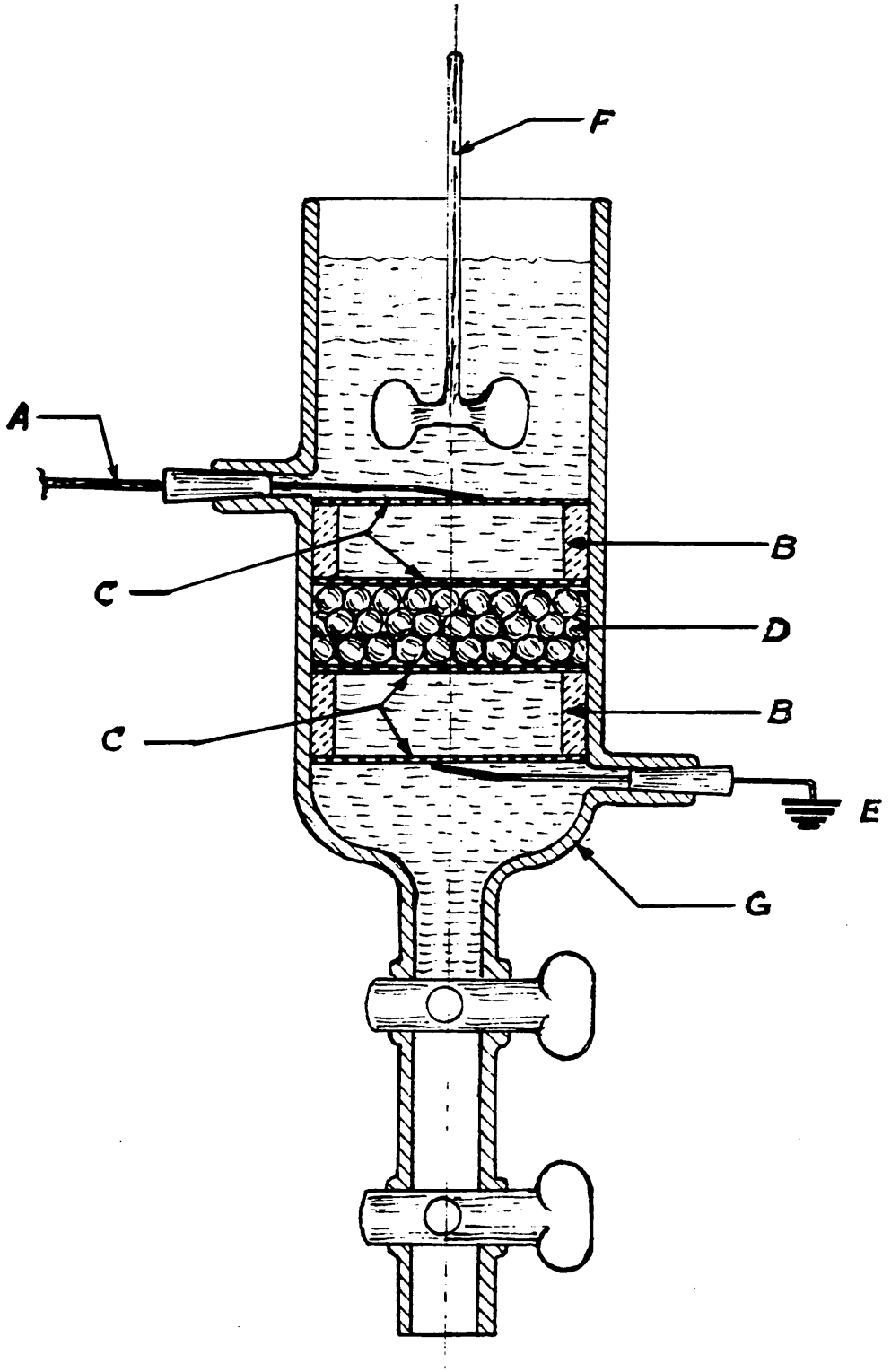

A is the live high voltage contact;
B are polythene insulating rings;
C are metal gauzes;
D is the area filled by spherical balls which act as matrix elements;
E is the earth contact;
F is the stirrer;
G is the glass vessel of radius 35 mm with a gap of 90 mm between the electrodes.

Figure 2.1.2. Apparatus for Matrix Element Tests in Uniform External Field.

d) Both products were washed in acetone to remove the dielectric liquid.

The kimberlite particles were of size -300 to + 212 μm and unless stated the liquid was not allowed to flow through the separator.

Four factors which could influence the separation were investigated:

1) The use of different matrix elements.
2) The strength of the externally applied electric/field.
3) The effect of the number of layers of matrix elements used.
4) The volume of sample treated.

2.1.5. Test Results

1) Comparison of the effects of steel and glass matrix elements in treating different volumes of kimberlite.

In these tests an applied voltage of 25 kV gave a field strength of 270 kV m^{-1}. Three layers of matrix elements were used.

Table 2.1.1. a. Test results for steel matrix elements with different sample volumes

Sample wt (g)	Sample Volume(cm^3)	Repelled		Attracted	
		Volume (cm^3)	% Volume	Volume (cm^3)	% Volume
20	6.9	0.44	6.4	6.46	93.6
25	8.62	0.48	5.5	8.14	94.5
30	10.35	0.76	7.3	9.59	92.7
35	12.07	1.00	8.3	11.07	91.7
40	13.80	1.15	8.3	12.65	91.7

Table 2.1.1. b. Test results for glass matrix elements with different sample volumes.

Sample wt (g)	Sample Volume(cm^3)	Repelled		Attracted	
		Volume (cm^3)	% Volume	Volume (cm^3)	% Volume
20	6.9	0.52	7.6	6.38	92.4
35	12.07	0.24	2.0	11.83	98.0
40	13.80	0.40	2.9	13.40	97.1
50	17.25	1.34	7.7	15.91	92.3

2) Effect of the applied external field using a fixed volume of particles with steel and glass matrix elements

Sample volume used = 6.9 cm^3 (20 g).

Table 2.1.1. c. Test results using different applied external fields with steel matrix elements.

Applied Voltage kV	Field strength kVm-1	Repelled		Attracted	
		Volume (cm^3)	% Volume	Volume (cm^3)	% Volume
0	0	6.67	96.6	0.23	3.4
5	55	2.75	39.9	4.15	60.1
10	111	2.84	40.1	4.06	58.9
15	166	1.39	20.1	5.51	79.9
20	212	0.84	12.2	6.06	87.8
25	277	0.44	6.4	6.46	93.6
30	333	0.23	3.3	6.67	96.7

Table 2.1.1. d. Test results using different applied external fields with glass matrix elements

Applied Voltage kV	Field strength kV m^{-1}	Repelled		Attracted	
		Volume (cm^3)	% Volume	Volume (cm^3)	% Volume
10	111	5.4	78.3	1.5	21.7
15	166	2.85	41.3	4.05	58.7
20	222	0.77	11.2	6.13	88.8
25	277	0.52	7.6	6.38	92.4

3) Effect of the number of layers of matrix elements used

Applied voltage = 25 kV (0.277 MVm^{-1})

Sample volume = 12 cm^3 (35 g)

Table 2.1.1. e. Test results using different numbers of layers of steel matrix elements

Number of layers	Repelled		Attracted	
	Volume (cm^3)	% Volume	Volume (cm^3)	% Volume
1	3.76	31.3	8.24	68.7
2	2.44	20.4	9.56	79.6
3	0.99	8.3	11.01	91.7

Table 2.1.1. f. Test results using different numbers of layers of glass matrix elements

Number of layers	Repelled		Attracted	
	Volume (cm^3)	% Volume	Volume (cm^3)	% Volume
1	4.46	37.2	7.54	62.8
2	3.14	26.2	8.86	73.8
3	0.24	2.0	11.73	98

4) Effect of liquid flow on the volume of particles retained

A single experiment was carried out at a field strength of 277 kV m^{-1} where the liquid was allowed to flow through the separator. The sample volume used was 6.9 cm^3 (20 g).

Table 2.1.1. g. Effect of liquid flow on the volume of particles retained

	Applied Voltage kV	Field Strength kVm^{-1}	Repelled		Attracted	
			Volume (cm^3)	% Volume	Volume (cm^3)	% Volume
With liquid flow	25	277	0.46	6.7	6.44	93.3
Without liquid flow	25	277	0.44	6.4	6.46	93.6

2.1.6. Discussion

The results show that which ever type of matrix is employed it is possible to attract kimberlite particles

given an adequate field strength. Tables 2.1.1. a + b show that there is no significant difference between steel and glass matrix elements (e.g. at a volume of 6.9 cm^3 with steel 93.6 % of the sample was repelled and with glass 92.4 %). This implies that individual particle/particle dipole interactions have some role to play in the process, because if only particle matrix interactions were important, there would be a larger attractive force using steel elements due to the difference in the steel to kimberlite relative permittivities being greater than for glass to kimberlite.

The percentage of particles attracted when the sample volume is high (e.g. glass matrix elements with a sample volume of 17.25 cm^3 gave 92.3 % attracted material) suggests there is a maximum sample volume treatable in one pass, due to mechanical trapping by particles already in the system. This means that any viable separation process would be intermittant requiring cyclic stoppage for sample removal. However, with only 3 % of a sample being held by mechanical means when there is no external field (e.g. between matrix elements on the electrodes, or between the matrix elements and separator walls) shows that particle attraction is likely to be due to particle-particle and particle-matrix Coulombic, rather than mechanical interaction.

Tables 2.1.1. c + d shows that when the field strength increases, so does the amount of attracted material. This is expected as the force on particles is proportional

to the square of the applied field [Equation 17] . At higher field strengths there is little difference in results using the two different matrix elements, although at both lower voltages [Tables 2.1.1. c + d] and different layers [Tables 2.1.1. e + f] steel gives better results than does glass. If it is assumed that particle-matrix interaction is a significant factor in the separation process than the greater difference in permittivities between steel and kimberlite and glass and kimberlite would give a greater attractive force. Whereas at higher field strengths [Table 2.1.1. a + b] particle-particle interaction is the predominant factor. Also if individual particle-particle interaction resulting in chains and clusters is the cause of particle attraction then the better results with steel would be due to the frictional stabilising effect of the matrix elements on chains and clusters, steel balls having a greater effect than glass balls. However, at larger field strengths this frictional effect becomes insignificant.

Table 2.1.1. g shows that liquid flow through the system has an insignificant effect on the amount of material attracted (93.3 % attracted with flow, 93.6 % without). This implies either that the liquid flowrate is insufficient to dislodge particles, or that due to the low volume of sample, there is enough space for the repeated capture of particles. This result is advantageous to any possible separation provided that

the liquid flowrate is sufficient to dislodge diamond particles and wash them through the system.

However for a complete understanding of the results, to decide whether particle/matrix or particle/particle interaction is the predominant factor in the separation process by calculating the forces involved and to show the precise nature of the zones of attraction and repulsion which arise on the matrix elements it is necessary to use the equations developed in Section 2.1.2.

2.1.7. Coulombic interaction forces arising between particles and matrix elements and between individual particles

Consider two sets of forces, those which arise between a kimberlite particle and a glass matrix element, and those which arise between individual particles. For the purpose of calculation, Equation (17) is used with the kimberlite particles being assumed spherical and of size 256 μm. The calculated numerical values are tabulated below in Table 2.1.2. and a full version of the calculations is shown in Appendix 1.

Table 2.1.2. Calculated numerical values of particle-particle and particle-matrix dipole dipole interaction forces

Externally Applied Voltage = 30 kV.

Field Strength E = 330 kV m^{-1}.

Particles involved	Diameter mm	Forces at Equator N m^{-3}	Forces at Poles N m^{-3}
Kimberlite particle Kimberlite particle	0.256 0.256	1730 (Attractive)	4193 (Repulsive)
Kimberlite particle Glass matrix element	0.256 12	81.9 (Repulsive)	110 (Attractive)

The data in Table 2.1.2. shows that in the particle separation process, the individual particle-particle interaction force is much greater than the particle-matrix element interaction force. For individual particles the equatorial attractive forces are twenty two times greater than the particle-matrix element polar attractive forces, whilst the polar repulsive forces are seventy three times greater than the particle matrix equatorial repulsive forces. This means that the formation of chains or clusters of particles between the electrodes is the main reason for the attraction process. It also explains the results given in Tables 2.1.1., which showed that there was no difference in the attraction/repulsion behaviour between steel and glass matrix elements due to the relatively small magnitudes of the particle-matrix element interaction force.

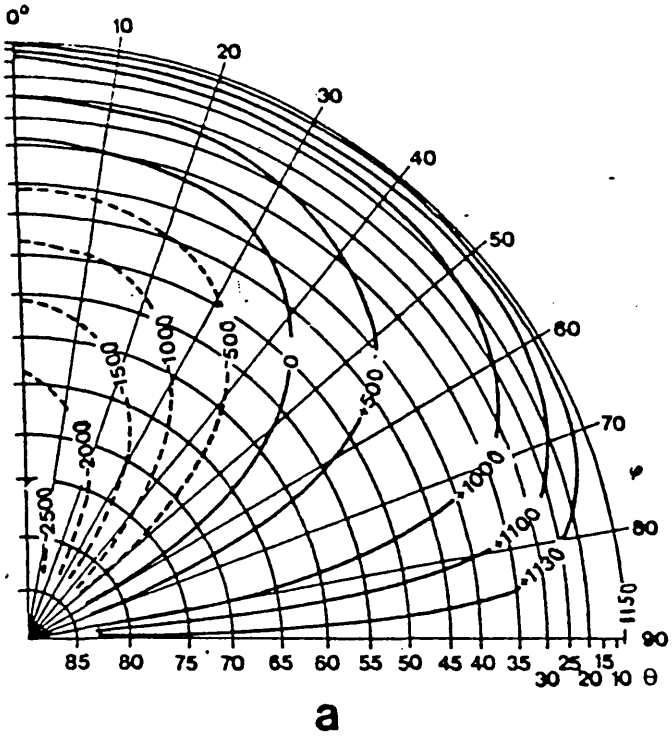

a

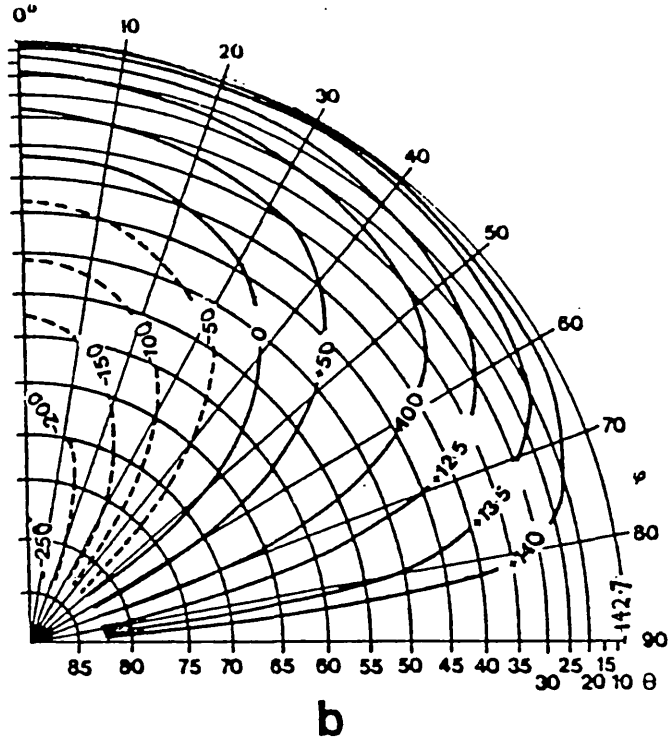

b

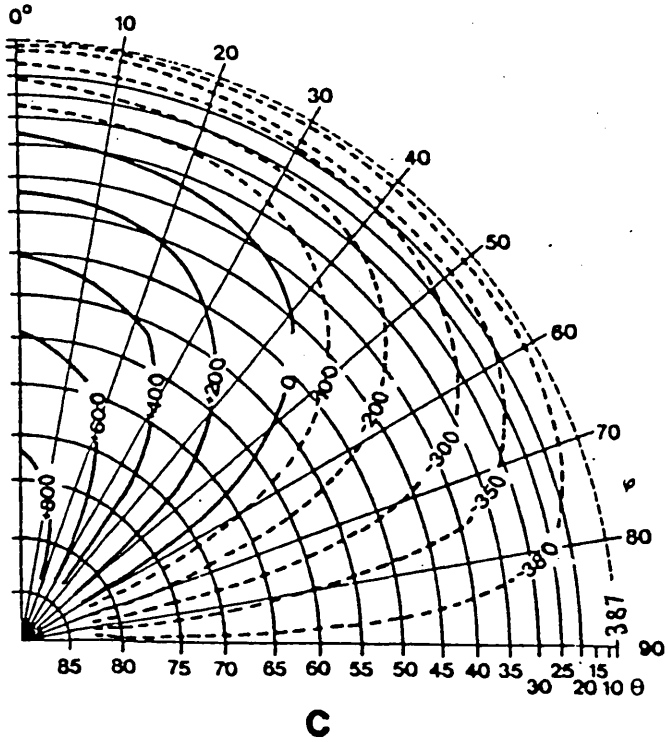

c

a - kimberlite - kimberlite particle

b - diamond - diamond particles

c - kimberlite - diamond particles

Figure 2.1.3. Pattern of the Radial Component of the Attraction Repulsion Force of Dipole-Dipole Interaction,

Further proof of the significance of individual particle-particle dipole interactions in the attraction process, can be derived from a consideration of the matrix elements attraction/repulsion zones, and also from the number of particle layers required tc attract all the particles, if particle attraction is solely due to particle matrix interaction.

2.1.8. Matrix element attraction-repulsion zones

Figure 2.1.3. shows lines of the radial component of the electrical force responsible for attraction-repulsion on the surface of a sphere. The calculations of the equipotentials using Equation (17) was carried out for a field of 1200 kV m^{-1} particle diameter 5 mm and taking the relative permittivities of kimberlite, diamond and liquid, as 7.4, 5.7 and 6.1 respectively. The forces are given in Nm^{-3}. The graphs (Figure 2.1.3) though not relating to the values of field strength and particle size used in the experiments, do give an indication of the relative values of forces involved and also of the position of particle attraction/repulsion zones.

The graphs show one quadrant of the distribution of forces viewed from the top of the sphere. Two symmetrical figure of eight areas can be distinguished in the vicinity of the sphere's poles. These curvilinear symmetrical areas are shown by dashed lines representing equipotential lines of repulsion, and by bold lines

which show the equipotential lines of attraction. In cases when particles are of identical material (kimberlite-kimberlite or diamond-diamond), the equatorial forces have values of maximum attraction, whereas for diamond-kimberlite the forces are of maximum repulsion.

Dipole-dipole interaction can only occur when the dielectric constants of both particles are higher or lower than that of the liquid medium. When the liquid has an intermediate dielectric constant relative to those of the particles, chaining and clustering is not possible because of the repulsion between particles.

According to equation (17), the radial force of attraction along the equatorial section of the sphere is eight times for kimberlite than for diamond. Thus chaining is most likely to occur for kimberlite particles only.

From a knowledge of the equipotential areas, it is possible to estimate the area of the matrix elements available for kimberlite attraction. Assuming only particle-matrix element dipole interaction, the number of particle layers formed may be calculated. For a kimberlite particle on glass, the solution of equation (17) such that the force F is zero gives the attraction/repulsion boundary shown in Figure 2.1.4. It can be seen that the actual area available for kimberlite attraction is quite small. This boundary is also the same for diamond attraction/repulsion onto glass, but

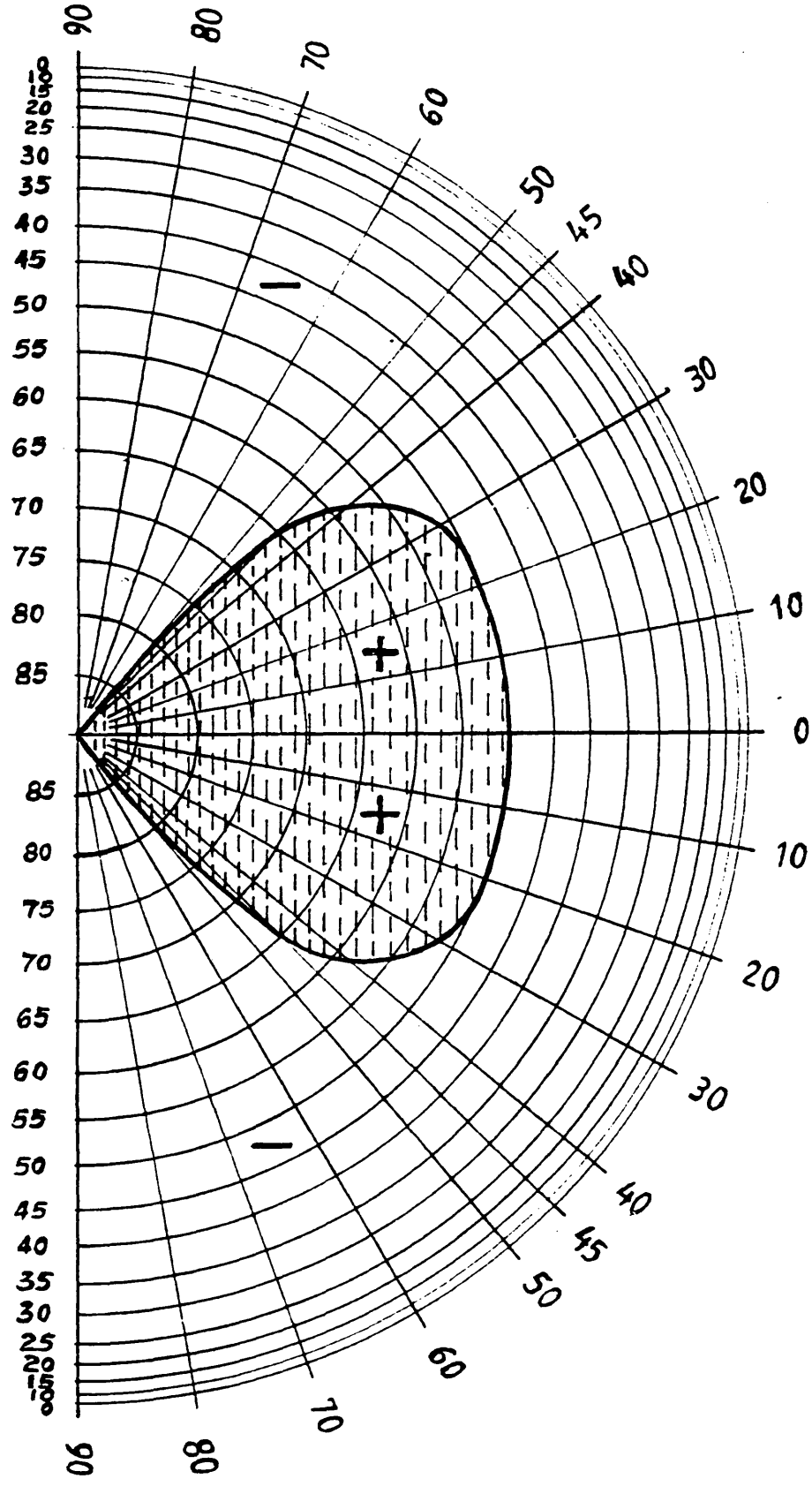

Figure 2.1.4. Attraction Repulsion Zones for Kimberlite Particles on Glass Matrix Elements.

where kimberlite is attracted, diamonds will be repelled and vice versa.

The precise size of the area of attraction is difficult to calculate. Let us assume that for a glass sphere only the top half is available for attraction/repulsion (due to the effect of gravity) and also that twenty five percent of the upper area of the sphere is available for attraction. Thus twelve and a half percent of the total area of a sphere is used for kimberlite attraction.

The experimental results can now be used to estimate the number of particle layers present assuming that only particle matrix element interaction is responsible for particle attraction. The data used for this calculation is that shown in Table 2.1.1.d. using different applied external fields.

Table 2.1.1. d. Test results using different applied external fields with glass matrix elements

Applied Voltage kV	Field strength kV m^{-1}	Repelled		Attracted	
		Volume (cm^3)	% Volume	Volume (cm^3)	% Volume
10	111	5.40	78.3	1.50	21.7
15	166	2.85	41.3	4.05	58.7
20	222	0.77	11.2	6.13	88.8
25	277	0.52	7.6	6.38	92.4

A table of the number of layers of kimberlite particles formed is shown below; a fuller version of calculations is shown in Appendix 2.

Table 2.1.3. Number of particle layers required for kimberlite matrix element attraction.

Applied Voltage kV	Field strength kV m-1	% Wt and % Volume Attracted	Volume Attracted cm^3	Weight Attracted (grams)	Number of Particles Attracted	Number of Particles layers
10	111	21.7	1.50	4.34	170866	2.46
15	166	58.7	4.05	11.74	462205	6.66
20	222	88.8	6.13	17.77	699606	10.09
25	277	92.4	6.38	18.48	727874	10.50

Several monolayers of particles must be formed on the matrix elements if particle attraction is due only to particle-matrix dipole interaction. Practically this means that, for example, at 25 kV with ten layers of 265 μm diameter particles, the total covering of particles formed would be 2 to 3 mm thick. It is difficult for such layers to exist, especially with the hexagonally close packed arrangement of the spherical matrix elements. This together with the relatively small forces between particles and matrix elements compared with those between individual particles, suggests that particle-particle interaction is the main reason for the dielectric attraction of kimberlite.

With a knowledge of the above figures, plots of attraction and repulsion zones and values of the relative forces involved, it was decided to confirm whether individual particle-particle or particle matrix dipole interaction was the dominant factor in this type of dielectric separation. Two sets of experiments, one to investigate particle-matrix element dipole interaction, the second particle-particle dipole interaction, were carried out to confirm the particle retention mechanism.

2.1.9. Experiments investigating mechanism of particle attraction

The first experiments investigating possible particle-matrix element dipole interaction involved observation of the behaviour of particles in the presence of a single matrix element polarised in a uniform field.

Two spheres were set up; the first a glass sphere of diameter 30 mm, specially blown for this experiment and the second was a steel (metal) ball also of diameter 30 mm. Both spheres were connected by gluing to the lower grounded electrode in the glass vessel shown in Figure 2.1.1. using a glass rod. The liquid used was Di-n-butyl phthalate with an applied potential of 600 V m^{-1}. The behaviour of the kimberlite particles with the glass sphere is shown in Plate 2.1.1. (a) and (b), Plate (b) showing the final equilibrium stage of the process.

There is no evidence of particle-matrix dipole interaction but the most important factor is individual particle-particle interaction. Indeed, the theory used for calculation of the zones of particle-matrix element interaction (Equation (17)) cannot be applied for steel matrix elements. Steel being a conductor.

There are several stages to the separation process. Initially the kimberlite particles are seen to move about in a seemingly random fashion before some come into contact at their equators. Then, due to tangential forces, particles orientate themselves in the direction

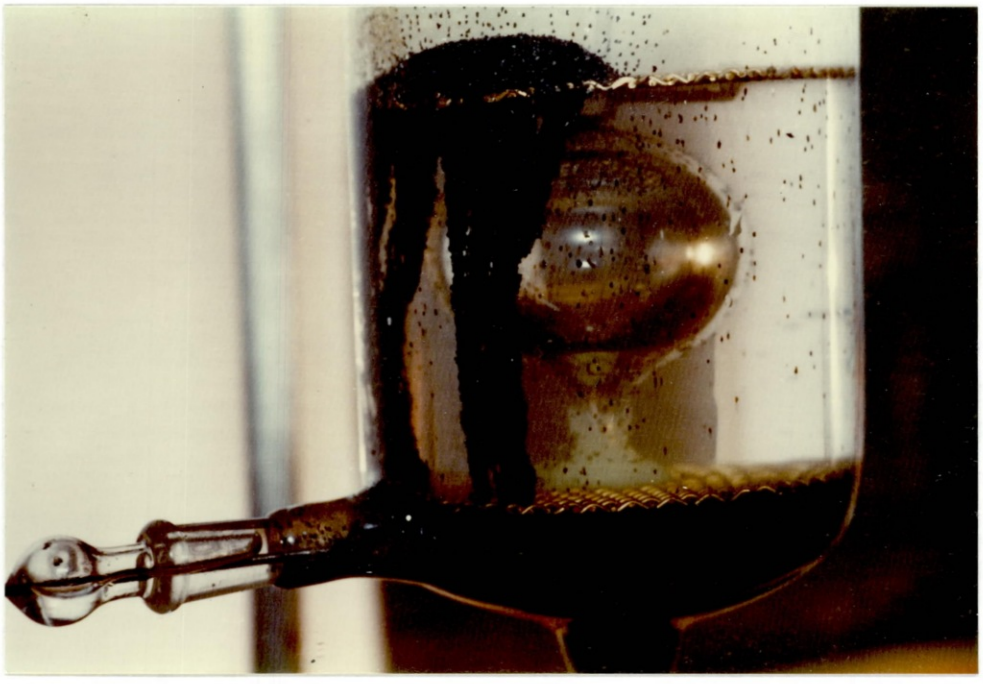

a)

b)

Plate 2.1.1. Particle Particle interaction in the presence of one matrix element.

of the external polarising field. This leads to the formation of chains of five to six particles. Some chains start from one of the two electrodes. The chains then grow until they bridge the two electrodes. The next stage is the formation of bunches which include several chains. This is due to chains attracting each other along their axes without distortion when the electrical field is increased above the necessary level for the initiation of chain formation. The shorter the distance between chains the more probable is their clustering. Particle/particle interaction is the first and most important process that occurs. The presence of matrix elements makes individual chains and clusters more stable due to friction between chains and matrix elements. This is confirmed by Tables 2.1.1. e and f which show that with the same applied field and sample volume the amount of material attracted increases with the number of matrix elements.

The experiments provide further evidence that particle-particle dipole interaction predominates in the attraction process. For confirmation a further series of experiments was carried out without matrix elements.

The liquids used were Di-n-butyl-phthalate and kerosene, with particles of kimberlite and quartz of size less than 1 mm. The applied potential was again 600 kV m^{-1}. The chaining process in kerosene is shown in Plate 2.1.2.

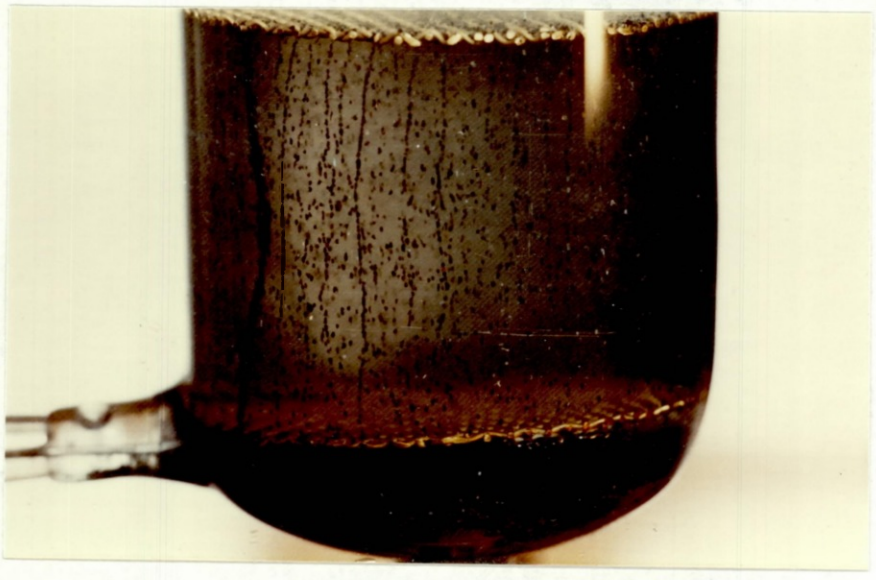

a)

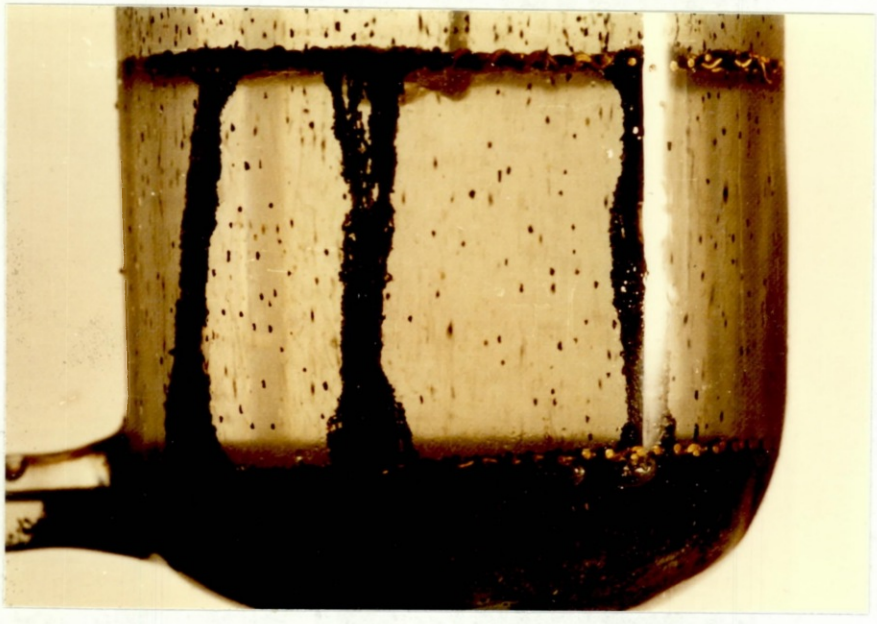

b)

c)

Plate 2.1.2. Chaining of Kimberlite Particles of size < 1 mm in kerosene. Quartz particles fall through without chaining.

The photographs show the transformation of chains (Photograph (a)) into bunches (Photographs (b) and (c)).

In kerosene, the kimberlite particles produce chains along the direction of the force lines, whilst the particles of quartz drop through the spaces between chains. The reasons for the non chaining of quartz can be seen from the relative magnitudes of the forces in equation (17).

Assuming that the particles of kimberlite and quartz are of equal size equation (17) shows that the force is 1.8 times greater for kimberlite particles than for similar quartz particles. This difference appears sufficient for forming chains by kimberlite but not by quartz. In kerosene the forces on particles are nine times smaller than in Di-n-butyl-phthalate, being proportional to the square of the dielectric constant of the liquid. Two other factors may influence this process. The quartz particles, were present in much smaller numbers than kimberlite particles, have less chance of coming into close enough contact to form chains and clusters. Repulsive equatorial kimberlite-quartz dipole-dipole interaction forces push individual quartz particles away from already formed kimberlite chains and so through the system.

In Di-n-butyl-phthalate similar phenomena are observed for kimberlite and quartz particles as in kerosene, although quartz particles might be expected to form chains

in this liquid. Calculations using equation (17) show that the dipole-dipole interaction forces on quartz are four times than those on kimberlite under similar conditions. Thus quartz-quartz dipole interaction forces should be of sufficient magnitude for chaining to occur. The only possible explanation for quartz particles not chaining is that they are present in insufficient numbers and do not come close enough for the larger interaction forces to be of any effect. For 1 mm quartz particles 5 mm apart the forces are of lesser magnitude than between two touching kimberlite particles. This non chaining is also aided by the kimberlite-quartz equatorial repulsive forces which tend to push individual quartz particles through the system.

The non-chaining of quartz particles in Di-n-butyl phthalate is a good pointer towards the application of this type of separator. It shows that even if particles can chain they will not do so unless present in sufficient quantities. Diamonds are present in very small numbers in kimberlite and diamond-diamond dipole-dipole interaction forces are one-eight of those which act on kimberlite particles (Figure 2.1.3). This suggests that a good separation of diamonds can be obtained with this system.

2.1.10. Summary of kimberlite attraction tests and mechanism of attraction.

The tests show that, with a separation system using matrix elements polarised in a uniform external field,

it is possible to attract and retain kimberlite particles provided that the applied external field and the number of layers of matrix elements are sufficiently large.

Kimberlite retention is not due to particle-matrix interaction but results from kimberlite-kimberlite interaction causing the formation of kimberlite chains and clusters. This has been shown by calculation of the respective magnitudes of the forces involved in kimberlite-kimberlite and kimberlite-matrix element interactions, as well as by experiments with single matrix elements and without matrix elements. However, matrix elements have a role to play in the separation process by making chains and clusters of kimberlite more stable.

2.1.11. Tests with kimberlite and glass mixtures.

Having shown that the separation system could attract and retain kimberlite particles, the next series of experiments was carried out to investigate whether the system could selectively separate a kimberlite and glass mixture by retaining kimberlite and repelling glass particles. For these tests a kimberlite/glass mixture containing 5 % glass by weight was used. Glass particles were used as a substitute for diamond because any separation obtained with glass should be more than equalled with diamond. According to equation (17), taking into account the differences in densities the forces of retention on glass particles should be twenty times greater than those for diamond.

2.1.12. Apparatus and procedure for mixture tests.

The test apparatus was similar to that of the previous experiments (Figure 2.1.2). Instead of polythene insulating rings, layers of glass and steel spheres were arranged between the two electrodes so as to prevent the current flow through the steel spheres which if of sufficient magnitude, would lead to breakdown of the electrical field. The additional layers of matrix elements, should increase the stability of the kimberlite chains and improve their retention by the system. The matrix elements were arranged as follows: Tests 1 to 4 used one glass layer, six steel layers and one glass layer. Tests 5 to 12 used alternate glass and steel layers with a glass layer at the bottom. Tests 13 to 15 used a similar arrangement but with a steel layer at the bottom.

The test samples consisted of 4.75 grams of kimberlite and 0.25 grams of glass in the -300 + 212 μm size range, 400 kV m^{-1}, this being the maximum possible under the tests conditions.

The test procedure was similar to that of the first set of experiments except that the dielectric liquid was allowed to flow through the system at a known rate. This liquid was necessary to wash glass through the system . Previous tests showed (Table 2.1.1.g) that the liquid flow does not seriously affect the amount of kimberlite retained by the system. Each test comprised a single pass of material through the system.

The separation results were analysed by heavy liquid separation (T.B.E) as tabulated below (Table 2.1.4). The kimberlite was pre-prepared to a density greater than 2.96 to simplify analysis.

Table 2.1.4. Results of single pass kimberlite glass separation tests.

Test Number	Quantity wash liquid (cm^3)	Liquid flowrate ($cm^3\ sec^{-1}$)	% Weight Material Repelled	% Recovery Glass	% Grade Glass
1	300	24	3.9	36	46
2	600	40	19.8	54	13.8
3	600	48	31	60	12
4	900	16	3.8	39	53
5	600	40	2.4	29.3	61
6	600	40	2.1	26	54
7	600	40	1.8	20.9	58
8	600	40	4.16	27.5	33
9	600	48	18.3	39	10.2
10	600	48	4.4	22.8	26
11	600	48	10.24	28.7	14
12	900	48	5.56	34.4	31
13	600	40	2.2	21.2	48
14	600	48	5.2	26	25
15	900	40	40.0	63	9

2.1.13. Discussion of Results.

Recovery and grade of the glass product show an inverse relationship. Increasing the liquid flowrate to raise the recovery of glass results in the washing out of weakly held kimberlite particles. The highest glass recovery of 63 % with a grade of 9 % is insufficient.

Tests 2 and 3 gave relatively high glass recoveries but at poor grades. The matrix arrangement of Tests 5 to 15 was adopted to hold the kimberlite particles more strongly. In test 2, using 600 cm^3 of liquid at a flow rate of 40 cm^3 sec^{-1}, 19.8 % material was repelled compared with 1.8 % - 2.4 % in tests 5, 6 and 7. However the alternative glass-steel arrangement lead to glass particles being more strongly held by the system. Recovery dropped from 54 % in test 2 to 20 - 29 % in tests 5, 6 and 7. Increased flowrates only increase recovery at the expense of grade.

Plate 2.1.3. shows a typical separation with alternate glass and steel matrix layers. The plate shows that particulate chains occur between the lower pole of one steel sphere and the upper pole of the steel sphere below it, implying that there is a stronger induced field through a glass sphere between a steel sphere and another steel sphere below, than between the two poles of one steel sphere. In the matrix of 1 glass, 6 steel, 1 glass layers, chains form from one electrode to another over a distance of up to 90 mm, whereas in the matrix of

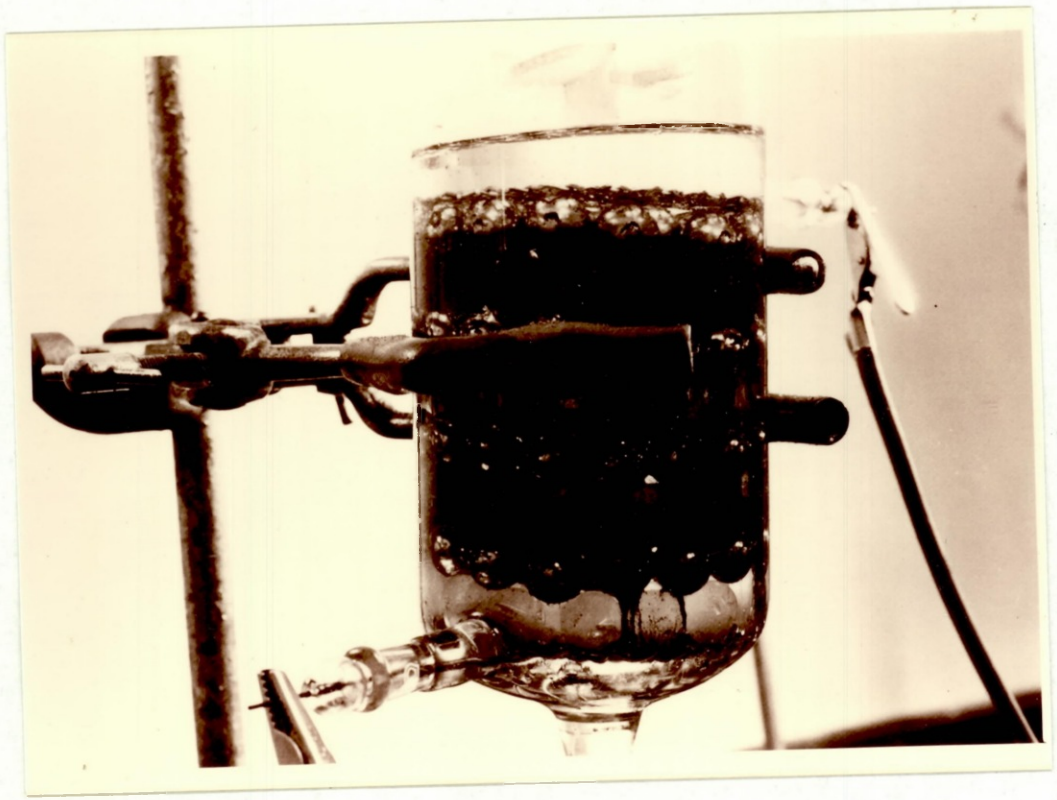

Plate 2.1.3. Matrix Separation using Alternate Glass and Steel Ball Arrangement.

Table 2.1.5. Comparative table of forces acting on kimberlite and glass particles

Externally Applied Voltage = 35 kV. Field strength E = 390 kV m^{-1}

Particles	Diameter (mm)	Forces at Equator (Nm^{-3})	Forces at Poles (Nm^{-3})
Kimberlite particle Kimberlite particle	0.256 0.256	2353 attractive	5702 repulsive
Glass particle Glass particle	0.256 0.256	9676.0 attractive	13004.0 repulsive
Kimberlite particle Glass matrix element	0.256 12.0	111.6 repulsive	149.9 attractive
Glass particle Glass matrix element	0.256 12.0	207.0 attractive	278.1 repulsive
Kimberlite particle Glass particles	0.256 0.256	5231.0 repulsive	12690.4 attractive

alternate layers chains are only about 10 - 15 mm long at the most. These shorter chains are much stronger and more stable. This may explain the increase in recovery compared with the one glass, six steel, one glass matrix.

At the bottom layer of glass spheres in Plate 2.1.3. the kimberlite chains do not necessarily contact the glass matrix elements. This appears to emphasise the prominence of particle-particle interaction in kimberlite retention. From the uppermost layer of steel balls there is no evidence of particle-matrix interaction, the only particles present being those trapped between the spheres and the separator walls.

2.1.14. Coulombic interaction forces involved and discussion of resutls.

It was noted (Section 2.1.9) that minority quartz particles in Di-n-butyl-phthalate would not form chains, despite dipole-dipole interaction forces for quartz being greater than for kimberlite. With glass particles the dipole dipole interaction forces are also greater than those which act on kimberlite particles, glass having a similar dielectric constant to quartz. The numerical values of the forces involved are tabulated below in Table 2.1.5. with a fuller version of the calculations being given in Appendix 3.

The forces acting on glass particles are about 2.5 times greater than those on kimberlite. Thus liquid flow through the separator will dislodge kimberlite particles from chains and clusters as well as glass particles as shown in the testwork.

Previous tests without matrix elements showed that small numbers of glass particles would not necessarily form chains. In these tests the quantity of glass is very small (.250 g occupies about 0.1 cm^3), but the presence of matrix elements in the system offers the glass particles a better chance of congregating in chains. These chains would be smaller and less stable than the kimberlite chains which contain large numbers of particles. Nevertheless some glass particles will be retained by the system.

Dipole-matrix interaction can be discarded in this separation as the forces on glass particles remain relatively small. Even if glass particles were held by matrix element attraction they would be washed off by the flow of liquid.

Finally the non-recovery of glass could be due to mechanical trapping of single or small bunches of particles by the more predominant kimberlite chains and clusters. Glass particles on top of a cluster could be held by the sheer number of kimberlite particles. In the next series of tests, using diamonds in a non uniform field, similar results were obtained as for glass. The forces on diamond are less than those acting on kimberlite

(according to Figure 2.1.3. one eight of the magnitude). This would suggest that mechanical entrapment as the main cause for non-selectivity.

The theory of separation in dielectric media had not been developed at the time of the testwork and it was thought that the retention of glass particles was due to particle-matrix interaction, glass particles being held at the equatorial region of the matrix elements. In order to investigate this, a series of separate tests was carried out using kimberlite and glass particles. (Table 2.1.6). The matrix consisted of alternate glass and steel layers with a glass layer at the bottom.

The test constraints were:

(i) Kimberlite and glass sample weights 5 grams;

(ii) Volume of Di-n-butyl phthalate wash liquid 700 cm^3;

(iii) Applied field 400 kV m^{-1};

(iv) Particle size range -300 + 212 μm.

Table 2.1.6. Results of separate sample tests.

liquid flowrate $cm^3 sec^{-1}$	Kimberlite		Glass	
	% Attracted	% Repelled	% Attracted	% Repelled
15.5	90.4	9.6	87.2	12.8
23.0	87.2	12.8		
24.0	86.3	13.7	80.1	19.9
46.4	78.7	21.3	63.0	27.0
48.0	71.0	29.0		

These results confirm the calculations shown in Table 2.1.5. and show that glass particles can chain when present in relatively large quantities. The results also show that the system and arrangement is suitable for particle attraction, but not for the selective repulsion of particles.

It may be concluded that the matrix hinders the free flow of glass particles through the system, allowing them to come into contact with each other and to be mechanically trapped by kimberlite particles. For working in a uniform field there are several possible alterations to the system. The matrix could be dispensed with, which would have a detrimental effect. It would slightly increase the amount of kimberlite repelled by losing the frictional attraction between the kimberlite and matrix elements. Alternatively,

the size of the matrix elements could be increased to allow a better flow of glass particles. This would create less chance of glass chaining or of mechanical extrapment by kimberlite chains. The separation could be carried out in kerosene or in a similar liquid of low dielectric constant where the forces are sufficient to cause chaining of kimberlite but not of quartz. By mixing Di-n-butyl phthalate and kerosene to give a dielectric liquid of the same constant as glass there would be zero force on glass particles, according to equation (17). The glass particles would fall freely through the system whilst kimberlite particles would be held in chains and clusters by dipole-dipole interaction.

However, at the time of the experiments it was thought that only particle-matrix element interaction forces are significant in the separation process. The next step was to increase the attraction forces on the kimberlite particles and to decrease those acting on glass particles. It was considered that a non-uniform external polarising field should provide a field gradient and hence a net force which could move particles in a direction dependent on their dielectric constant relative to the dielectric liquid medium. Kimberlite particles should move up the gradient towards higher forces, glass particles should move down the field gradient towards lower forces.

2.2. Separation tests using matrix elements in a non-uniform polarising field.

2.2.1. Introduction and Theory

The transitional force which acts up or down the gradient of a non-uniform, external, polarising field would be additional to the particle-particle and particle -matrix forces. The field gradient results in a difference between the Coulombic forces which act on opposite poles of a solidparticle as shown in Figure 2.2.1.

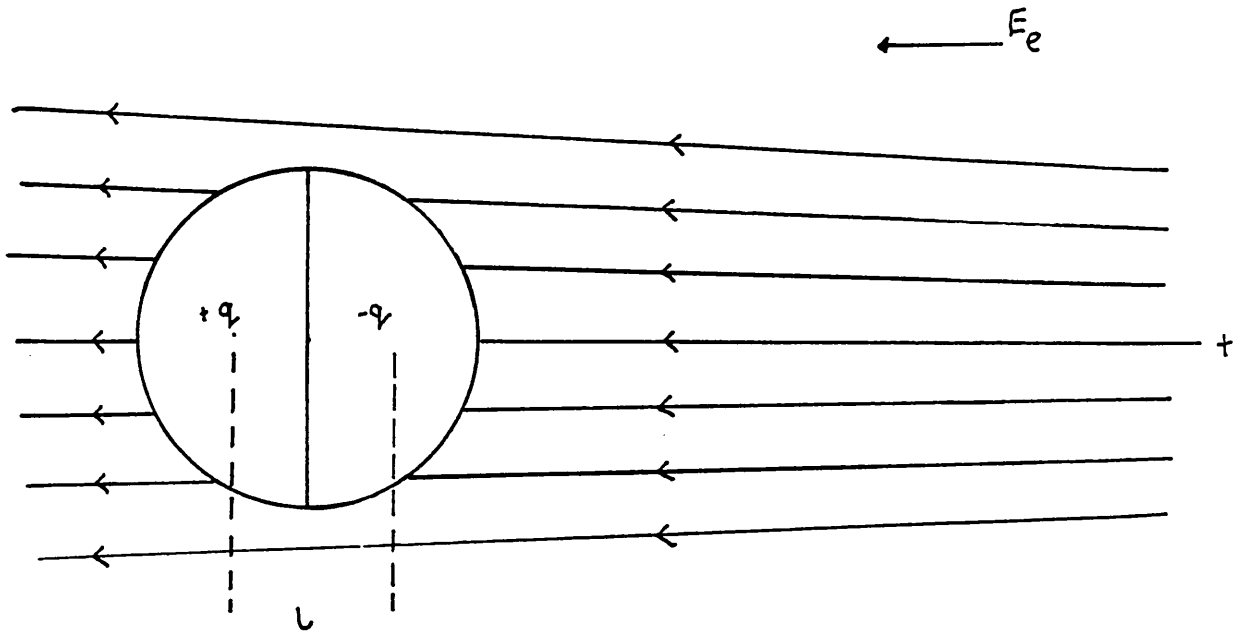

Figure 2.2.1. Spherical Particle in a Non Uniform Polarising Field.

The difference in the Coulombic forces yield an expression for the net force on a particle immersed in a dielectric liquid:

$$Fx = -qE + q(E + l\frac{dE}{dx}) = q\, l\frac{dE}{dx} = p\frac{dE}{dx} \qquad (20)$$

q is the charge of a particle, E is the applied external field and p is a dipole moment of the particle.

The dipole moment of a dielectric sphere is given by:

$$p = E.\ 4\pi\xi_o\varepsilon_L\ \frac{\varepsilon_p - \varepsilon_L}{\varepsilon_p + 2\varepsilon_L}\ .\ R^3$$

The force acting along the electrical field is

$$Fx = 4\pi\varepsilon_o.\varepsilon_L\ \frac{(\varepsilon_p - \varepsilon_L)}{(\varepsilon_p + 2\varepsilon_L)}\ R^3\ \text{grad}\ E^2 \qquad (21)$$

Equation (21) shows that the sign of $(\varepsilon_p - \varepsilon_L)$ will determine the direction of the force: $(\varepsilon_p - \varepsilon_L)$ is positive for kimberlite, but negative for glass and diamond. Thus in Figure 2.2.1. kimberlite particles with be deflected to the right, into the higher part of the field whilst glass and diamond particles will be deflected to the left into the lower part of the field.

The aim of using a non uniform field is to deflect kimberlite particles into an area where the field is more concentrated. This increases the dipole-dipole forces between the kimberlite particles and they will be more strongly held by the system. For glass or diamond the motion will be towards the weaker part of the field, decreasing the dipole-dipole interaction forces between those particles. The movement of kimberlite and glass particles in opposite directions should also tend to decrease the hazard of mechanical entrapment.

2.2.2. Experimental

The separation vessel used for this work is shown diagramatically in Figure 2.2.2. The weights and proportions of kimberlite and glass particles were the same as for tests in the uniform field (Section 2.1.12).

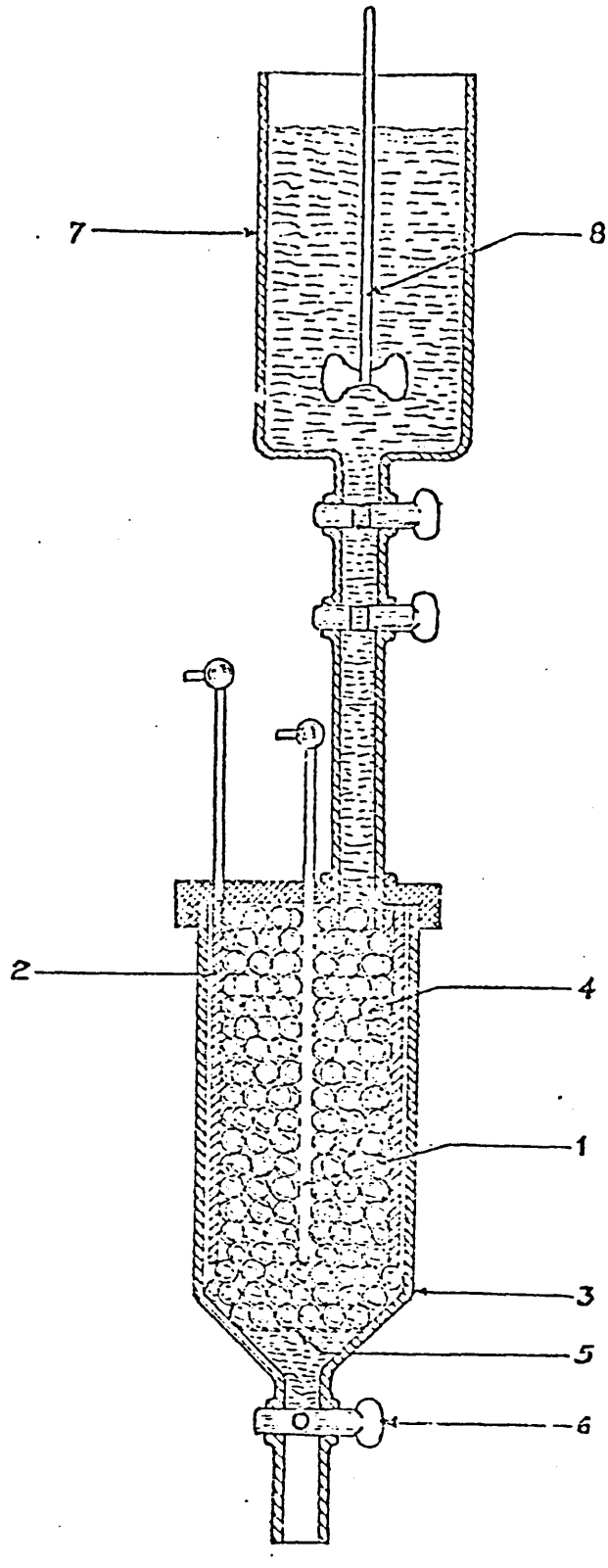

KEY

1. The Central Live Electrode
2. The Outer Grounded Electrode
3. The Glass Separating Vessel
4. The Matrix of Glass Balls Diameter 12mm
5. A Metal Gauze to support the Matrix Elements
6. The Discharge tap for Separated Products and Liquid
7. The Upper Glass Reservoir for Wash Liquid and Feed
8. The Stirrer for Dispersing the Feed

Figure 2.2.2 Apparatus for Matrix Element Tests in a Non-Uniform Field

The field strength was 1000 kV m^{-1}, the maximum for the available equipment. Only glass matrix elements were used as it would have been impossible to arrange a system of glass and steel elements which would not provide a conductive path of steel balls between the electrodes. The test results are tabulated below in Table 2.2.1.

The results show that the system achieves particle attraction but fails to attain adequate selective repulsion. The results for glass are better than corresponding ones in a uniform field both for grade and for recovery. Comparison of tables 2.1.4. and 2.2.1. shows that at a wash liquid volume of 900 cm^3 and at a flowrate of 48 cm^3 sec^{-1}, the uniform field yielded 34 % of the glass at a grade of 31 %. In the non-uniform field 900 cm^3 of wash liquid at 16 cm^3 sec^{-1} 32 % of the glass was recovered at a grade of 71 %.

The retention of two-thirds of the glass particles may be due to several factors. It is difficult to develop equations for calculating the relative magnitudes of forces in a non-uniform field. It may be justifiable to assume that particle-particle effects predominate over particle-matrix effects in dipole-dipole interaction. Particle chains would have to form in a horizontal direction. Although this seems unlikely, such chains have been observed in later tests with an isodynamic field in the vertical mode. The same effect should occur in this system, especially with the additional frictional

Table 2.2.1. Results of separation tests in a non-uniform field using kimberlite/glass mixtures

One pass only.

Wash liquid volume/cm^3	Flowrate cm^3 sec^{-1}	Attracted Material			Repelled Material		
		% Wt	% Grade Glass	% Recovery Glass	% Wt	% Grade Glass	% Recovery Glass
1000	26	85.40	2.87	46	14.6	24.0	54.0
900	4	99.15	4.40	92.0	0.85	43.0	8.0
900	16	98.30	3.70	68.0	1.70	71.0	32.0

In addition to the kimberlite/glass separation tests a single experiment was carried out with a kimberlite diamond mixture of wt 5 g and containing 0.95 % diamond by weight. (Table 2.2.2).

Table 2.2.2. Kimberlite/diamond separation test in a non-uniform field.

One pass only.

Wash liquid volume/cm^3	Flowrate cm^3 sec^{-1}	Attracted Material			Repelled Material		
		% Wt	% Grade Diamond	% Recovery Diamond	% Wt	% Grade Diamond	% Recovery Diamond
850	16	98.8	0.67	71	1.2	20	29

stability due to the matrix elements. Kimberlite particles could be deflected radially so as to be deposited on the circular outer electrode.

The dipole-dipole interaction may be significant for the glass particles. There is very little free space between individual matrix elements, giving glass particles more probability of contact although the movement into the weaker part of the field would weaken the dipole-dipole interaction forces. In addition deflected glass particles may bedeposited on the inner electrode. However the main factor in the retention of glass particles is indicated by the diamond separation test. The forces acting on diamonds are one eigth of those acting on kimberlite, thus it may be assumed that dipole-dipole interaction between diamond particles is insignificant. However there is no significant improvement in the recovery of diamond compared with glass. This suggests that mechanical trapping, either between matrix elements or by kimberlite clusters, is the main reason for the retention of quartz and of diamonds in both uniform and non-uniform external fields. It was concluded that recovery might be raised by improving the flow of glass or diamond through the system.

2.2.3. Possible modifications to separation system.

The beneficial deflection of particles in the divergent field suggested that mechanical entrapment might be reduced further by increasing the separator length to give particles more opportunity of separating. An increase in the size

of the matrix elements should allow freer passage of glass particles, but this would need to be balanced so as to maintain adequate retention of kimberlite.

A more radical approach would be to dispense with the matrix and to rely solely on selective displacement in opposite directions to achieve a continuous separation of the mixture. A circular feeder ring could be placed between the two electrodes and a fixed or movable annular splitter could be used at the bottom of the separator. A sketch of such a system is shown in Figure 2.2.3. Other design factors would be the length and width of the separator. The length must allow sufficient time for complete separation of the free-falling particles. The width of the separator should permit particle displacement without deposition on the outer electrode. Deposition of kimberlite on the inner electrode may necessitate cyclic cleaning.

In view of the non-uniform deflection of glass or diamond particles it might be better to position the feeder over the area where diamonds would be recovered. The separation, would then rely more on the stronger deflection of kimberlite particles.

2.2.4. Summary and conclusions of matrix tests.

Dielectric separation tests with matrix elements in uniform and non-uniform polarising fields were successful in the retention of particles which have dielectric constants higher than that of the liquid. The expulsion

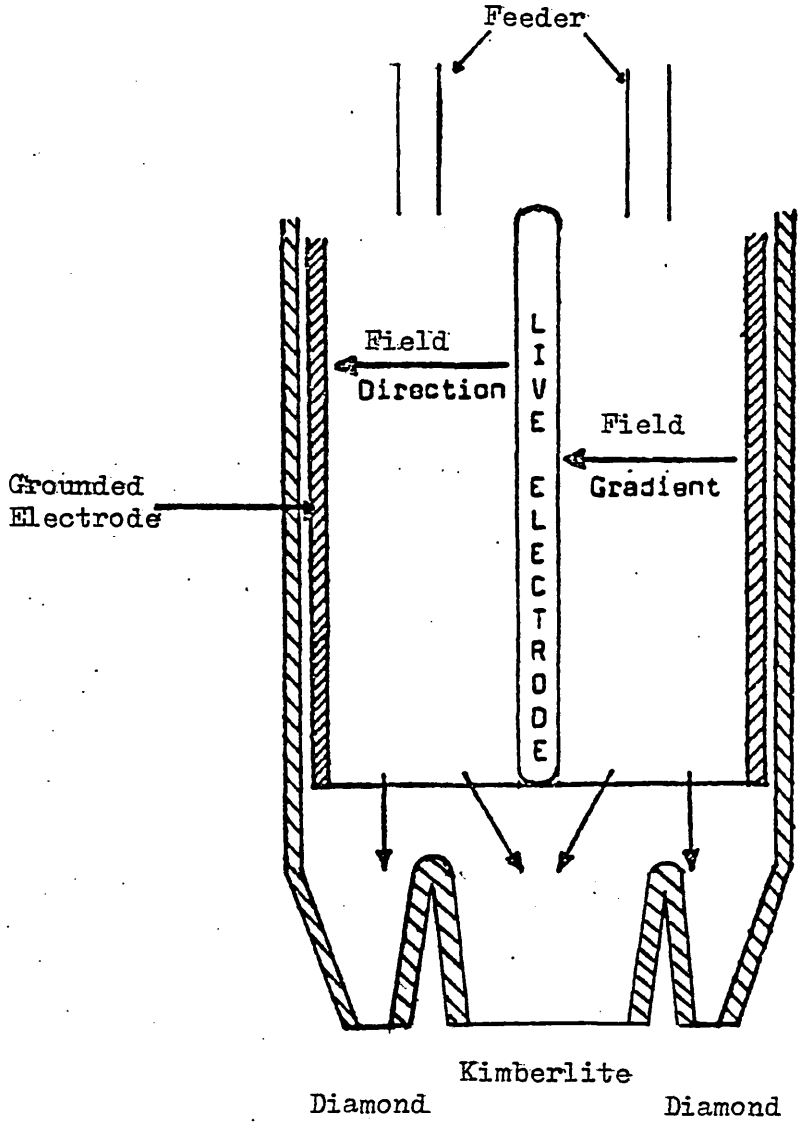

Figure 2.2.3. Selective Displacement Separation System in Non-uniform Field.

of particles with low dielectric constants was less successful due to mechanical trapping of particles in the system. Particle-particle dipole-dipole interaction is regarded as the dominant mechanism in obtaining a separation through specific chaining or non chaining of particle types in a uniform field.

A divergent field yields improved separation due to selective spatial displacement. Particles with higher dielectric constants than the liquid move up the field gradient and those with lower dielectric constants move down the field gradient across the direction of particle travel. The possibility of working continuously with a non uniform field and without a matrix has been indicated.

Chapter 3. DIELECTRIC SEPARATION USING DIFFERENTIAL DISPLACEMENT

3.1. Basis and theory

The displacement force in a non-uniform electrical field depends on the field configuration. In an electrical field of spherical symmetry, between two concentric spherical electrodes, the magnitude of the displacing force is

$$f = Kr^{-5} \tag{22}$$

r is the radial distance between the two spheres.

For an electrical field of cylindrical symmetry the displacing force is

$$f = K_1 r^{-3} \tag{23}$$

r is the radial distance between two corcentric cylinders. For an electrical field of hyperbolic symmetry the corresponding force is

$$f = K_2 r \tag{24}$$

r is the distance between the centre of the coordinates and a point on the axis of symmetry.

In order to balance a uniform gravitational force, it is desirable to use a uniform electric force throughout the separating zone. This is provided by an isodynamic field which is characterised by the following expression

$$EVE = \text{constant} \tag{25}$$

Without electrical current flows or if the current is negligable, the Laplace equation for the potential of the electrical field V is

$$\nabla^2 V = 0 \tag{26}$$

The solution of this equation in cylindrical co-ordinates is

$$V = Ar^n \sin(n\theta) \tag{27}$$

Here A is a constant and r and θ are co-ordinates since the electrical field is $-\nabla V$,

$$E = -(dV/dr)J_r - 1/r(dV/d\theta)J_\theta \tag{28}$$

Substituting (27) into (28)

$$E = -nAr^{n-1}[J_r \sin(n\theta).J_\theta \cos(n\theta)] \tag{29}$$

Here J_r and J_θ are unit vectors so

$$E^2 = n^2A^2r^{2(n-1)} \tag{30}$$

The displacing force is

$$F = -p\nabla E = -4\pi\varepsilon_o\varepsilon_\ell \frac{(\varepsilon_p-\varepsilon_\ell)\ r^3}{(\varepsilon_p+2\varepsilon_\ell)} . \tfrac{1}{2}\nabla E^2 \tag{31}$$

The force per unit volume is

$$f = \frac{F}{(4/3)\pi R^3} = -3\varepsilon_o\varepsilon_\ell \frac{(\varepsilon_p-\varepsilon_\ell)}{(\varepsilon_p+2\varepsilon_\ell)} . \tfrac{1}{2}\nabla E^2 \tag{32}$$

Substituting (30) into (32)

$$f = -3\varepsilon_o\varepsilon_\ell \frac{(\varepsilon_p-\varepsilon_\ell)}{(\varepsilon_p+2\varepsilon_\ell)} . \tfrac{1}{2} \frac{2(n-1)n^2A^2r^{2(n-1)}}{r} \quad J_n =$$

$$= -3\varepsilon_o\varepsilon_\ell \frac{(\varepsilon_p-\varepsilon_\ell)}{(\varepsilon_p+2\varepsilon_\ell)} (n-1)n^2A^2r^{2n-3} \quad J_n \tag{33}$$

Here ε_ℓ and ε_p are the relative permittivities of the liquid and particles respectively. ε_o is the permittivity of free space = 8.86×10^{-12} Fm^{-1} = $1/36\pi \times 10^{-9}$.

For an isodynamic field the force is independent of the radius vector (along radius r)

Then

$$r^{(2n-3)}=1 \tag{34}$$

and

$$2n-3 = 0 \tag{35}$$

Thus the exponent $n = \frac{3}{2}$

The constant A can be found by rearranging (33) and is

$$A = \tfrac{g}{3}\left(\tfrac{2}{3}f \frac{(\varepsilon_p+2\varepsilon_\ell)}{\varepsilon_o \varepsilon_\ell (\varepsilon_p-\varepsilon_\ell)}\right)^{\frac{1}{2}} \tag{36}$$

The distance between the geometric centre of the electrode system and the surface of the isodynamic field is

$$r = r_{60^o} (\sin \tfrac{1}{2}\theta)^{-2/3} \tag{37}$$

The lines obeying this relationship are shown in Figure 3.1. The squared gradient of the isodynamic field is

$$\nabla E^2 = \frac{9}{4} V^2/r^3_{60^o} \tag{38}$$

Thus substituting (38) into (33)

$$f = -\frac{3}{2}\varepsilon_o \varepsilon_\ell \frac{(\varepsilon_p-\varepsilon_\ell)}{(\varepsilon_p+2\varepsilon_\ell)} \nabla E^2$$

$$= -\frac{3}{2} \frac{\varepsilon_o \varepsilon_\ell (\varepsilon_p-\varepsilon_\ell)}{(\varepsilon_p + 2\varepsilon_\ell)} \cdot \frac{9}{4} \frac{V^2}{r^3_{60}} \tag{39}$$

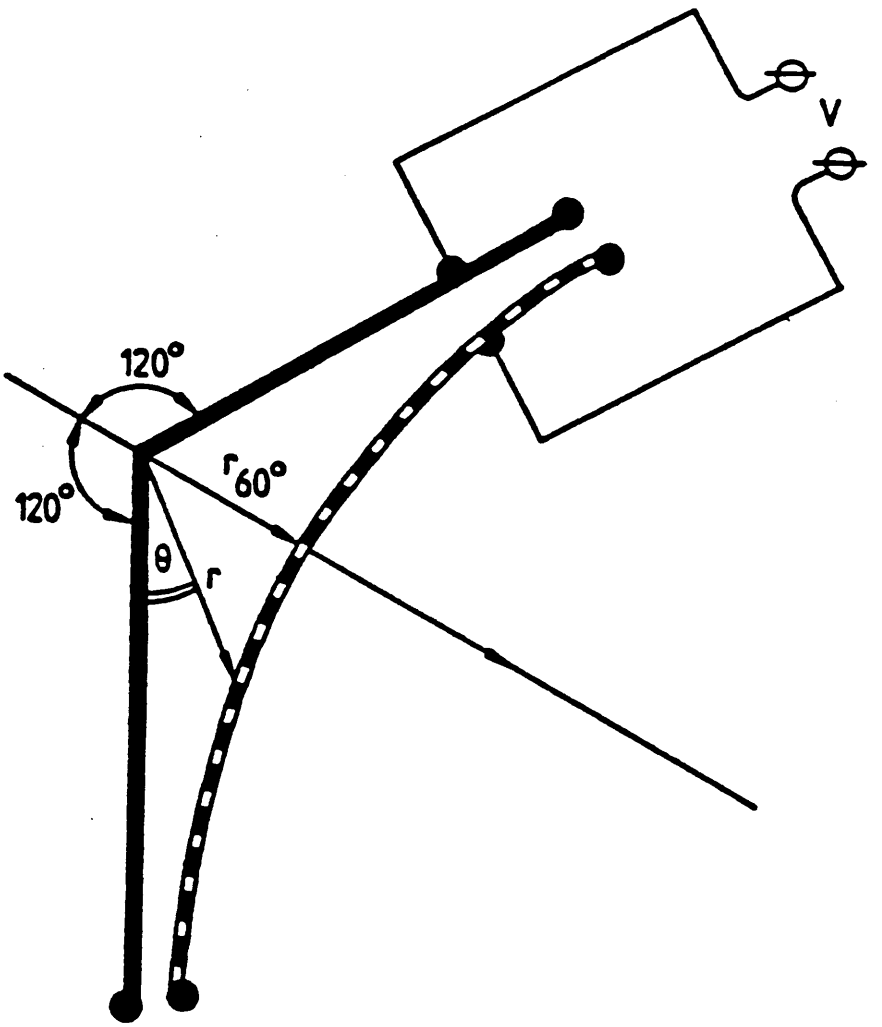

Figure 3.1. Isodynamic Electrodes.

3.2. Modes of dielectric separation

Equation (39) gives the dielectric force which acts on a particle during the separation. In order to separate two minerals purely on the basis of difference in their permittivity, the suspension of particles would have to be carried with a velocity higher than the terminal velocity of the particles. Normally the separation results from the joint action of electrical and gravitational forces. The electrical force is proportional to the permittivity differential between particles and liquid and to the squared potential of the electrical field. The gravitational force is proportional to the density differential of the minerals in the liquid and to the gravitational acceleration. The fluid resistance to particle displacement also needs to be taken into account.

Selective particle deflection can occur either in free fall or in horizontal transportation. The latter can be arranged through the forced flow of a liquid dielectric through the electric field, or through vibrational transportation of the solids in a stationary dielectric medium.

For both modes of separation the basic balance of forces is

$$\bar{f} = \bar{f}e + \bar{f}g + \bar{f}r \qquad (40)$$

$\bar{f}e$ is the electrical force, $\bar{f}g$ is the gravitational force and $\bar{f}r$ is the force of resistivity.

In the case of free fall or hydraulic transportation by vertical or horizontal flow of a liquid dielectric, $\bar{F}r$ is equal to the drag force and depends on the Reynolds number prevailing for the moving particles.

3.3. Separation with horizontal vibrational transportation

3.3.1. Tests with simple particles and with arbitrary mixtures

The principle of isodynamic separator was tested in a small scale device with a working volume of 70 cm^3 (Figure 3.2.) Consistent differential displacement was achieved depending on the differential dielectric constant. Diamonds ($\varepsilon_p - \varepsilon_\ell < 0$) move down gradient and kimberlite ($\varepsilon_p - \varepsilon_\ell > 0$) move up gradient as indicated in Figure 3.2.

A larger system was built with a profiled electrode 440 mm long and 70 mm wide (Plate 3.1). This electrode was first mounted horizontally on a vibrating feeder for moving the particles in a glass box over a flat electrode. The separator had a minimum working gap of 35 mm.

Initial experiments were carried out with mixtures of minerals prepared by D.R.L. These minerals were diamond, quartz, white zircon, brown zircon, ilmenite, diopside, unaltered and altered garnet, pyrite, calcite and kimberlite. Relatively large numbers of particles (500 to 1500) were used in one pass. It was observed that selective chaining and clustering occured, similar to the behaviour in the presence of matrix elements. Chain movement occurs when the potential is sufficiently high. The chains are stable and break up only at the

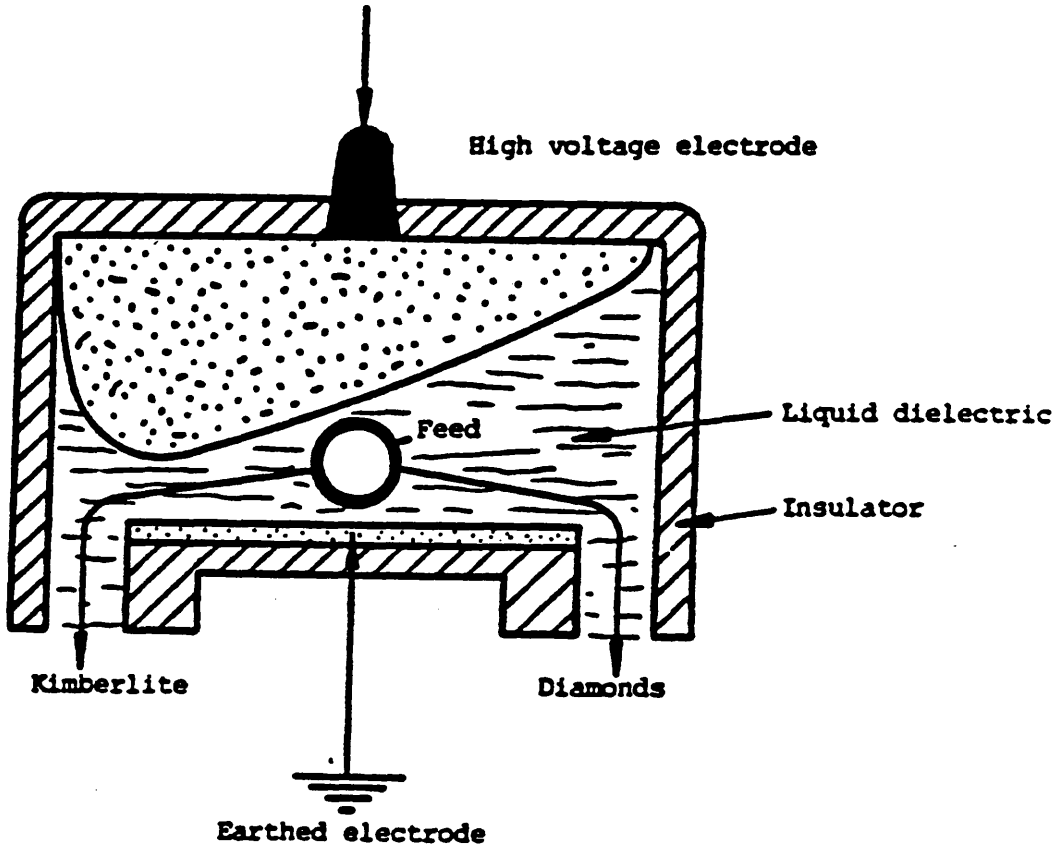

Figure 3.2. Isodynamic Dielectric Separator.

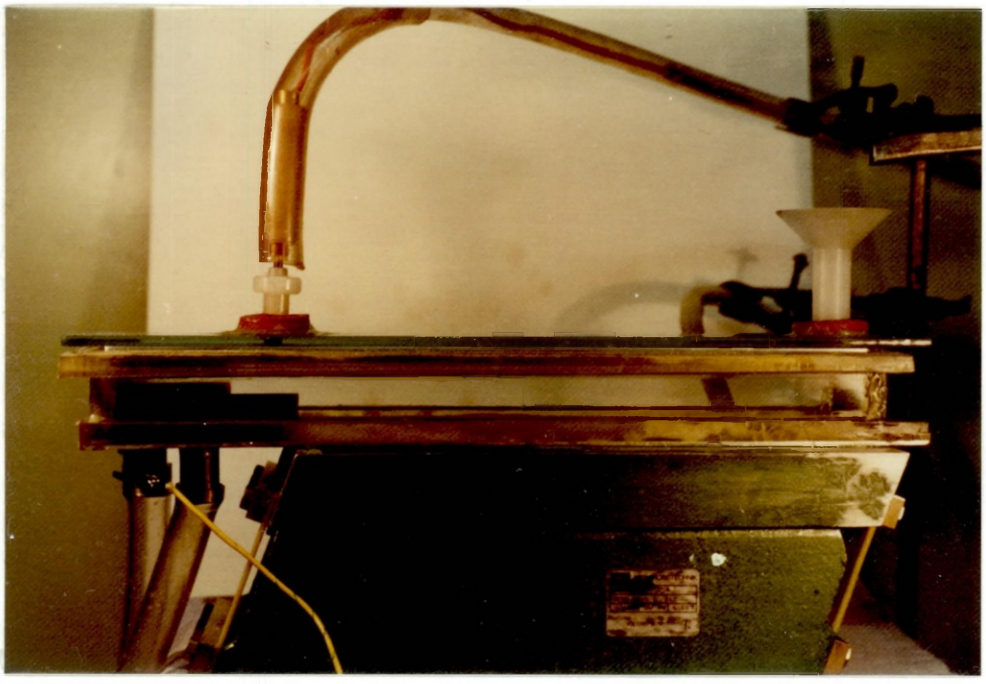

Plate 3.1. Horizontal mode of Dielectric Separation.

discharge orifice.

Chaining occured only for particles with $\varepsilon p > \varepsilon_{\ell}$. The formation and movement of chains in the correct direction was an advantageous factor for the treatment of large quantities of material by making better use of the space between the electrodes. It is a disadvantage that the chains occasionally conduct current when the intermittent reduction of the liquid film between particles creates contact between the two electrodes along the chains. The momentary drop in the applied electrical field reduces the force on the particles. A possible solution might be the insertion of a porous division between the two electrodes, allowing the passage of liquid and not effecting the field.

It was observed that diamonds are never involved in chains, presumably due to the low magnitudes of dipole-dipole interaction. In over a dozen separation tests, all diamonds were recovered in the concentrate. This 100 % recovery could be due firstly to high density and shape stabilising movement and secondly the low difference in dielectric constant producing low speed of travel. Both factors result in longer residence time in the separator with a better chance of separation.

Table 3.3.1. shows typical separation results obtained in the horizontal channel at a voltage of 1340 kV m^{-1} (The maximum obtainable from the high voltage transformer).

Table 3.3.1. Treatment of a mixed mineral assembly in the horizontal channel

Material	Number of particles in feed	First Pass		First Retreat		Second Retreat		Third Retreat		Fourth Retreat	
		Concentrate %	Total Tail%	Concentrate %	Total Tail%	Concentrate %	Total Tail%	Concentrate %	Total Tail%	Concentrate %	Total Tail%
Diamond	6	100	0	100	0	100	0	100	0	100	0
Quartz	100	72	28	30	70	23	77	10	90	8	92
White Zircon	100	53	47	22	78	15	85	10	90	8	92
Brown Zircon	100	48	52	19	81	18	82	8	92	5	95
Ilmenite	100	22	78	5	95	2	98	1	99	1	99
Diopside	100	20	80	9	91	3	97	0	100	0	100
Garnet (Unaltered)	100	45	55	20	80	10	90	5	95	3	98
Garnet (Altered)	100	15	85	1	99	0	100	0	100	0	100
Pyrite	100	25	75	1	99	0	100	0	100	0	100
Calcite	100	52	48	31	69	23	77	13	87	9	91
Kimberlite	100	21	79	7	93	2	98	0	98	0	100
Total	1006	38.2	62.4	15.1	84.9	9.9	90.1	4.6	95.4	3.4	96.6
Grade Diamond %	0.6	1.60		4.0		6.0		12.0		15.0	

Amongst the 10 minerals two groups can be distinguished according to their separability (Table 3.3.2).

Table 3.3.2. Separability of Minerals

High Separability	Low Separability
-Diamond	-Quartz
+ Ilmenite	+Zircon
+ Diopside	+Garnet(Unaltered)
+Garnet(Altered)	+Calcite
+Pyrite	
+Kimberlite	

The positive sign indicates that the minerals is deflected up-gradient towards the higher field intensity and the negative sign indicates deflection down-gradient towards the lower field intensity.

The low separability of quartz is interesting. Although quartz should behave like diamond, only 70 % of the quartz is recovered with 100 % of the diamonds. Thus Table 3.3.1. shows that after 5 passes only 8 % of the quartz remains with the diamonds. This behaviour of quartz may be due to combined shape and density effects, or it could be caused by surface forces.

As the majority of the feed particles is moving into one product slot minority particles which are moving feebly towards the other product slot can be trapped mechanically. This could be ameliorated by using a lower feed rate or a wider channel so as to

reduce the volumetric concentration of particles. Similarly the separation could be improved by reducing the rate of vibration and hence increasing the residence time in the separator.

3.3.2. Separation of industrial feeds

Following the work with arbitrary mineral mixtures, tests were carried out to investigate the behaviour of "real", alluvial materials. Two samples of normal feed for hand sorting at the Kleinsee mine were treated at a field strength of 1270 kV m^{-1}, followed by a single retreatment of the first concentrate. In accordance with normal industrial practice, the samples were closely sized to -7 + 5mm and -5 + 2 mm respectively. The coarser sample contained 3 diamonds in a total of 770 particles. The finer sample contained 1 diamond in a total of 1060 particles. Results are shown in Tables 33.3 and 33.4.

Table 3.3.3. Separation of Kleinsee pre-concentrate (-7 + 5 mm) from the bulk sampling plant.

Product	1st Pass		2nd Pass		Total	
	% by Number		% by Number		% by Number	
	Diamond	Total Material	Diamond	Total Material	Diamond	Total Material
Feed	0.39	100.0	1.56	24.8	0.39	100.0
Concentrate	1.56	24.8	8.60	5.8	8.60	5.8
Tailings	0.00	75.2	0.00	19.0	0.00	94.2

After two passes 94.2 % of the feed particles was rejected and all three diamonds were recovered in the remaining 5.8 % with an increase in grade from 0.39 % to 5.8 %. Although this is highly satisfactory, the result of a simple test with such small numbers of diamonds cannot be regarded as proof of separation efficiency.

Table 3.3.4. Separation of Kleinsee pre-concentrate (-5 + 2 mm) from the bulk sampling plant.

Product	1st Pass		2nd Pass		Total	
	% by Number		% by Number		% by Number	
	Diamond	Total Material	Diamond	Total Material	Diamond	Total Material
Feed	0.094	100.0	0.410	23.2	0.094	100.0
Concentrate	0.410	23.2	2.44	3.8	2.44	3.8
Tailings	0.000	76.8	0.00	19,4	0.00	96.2

After two passes 96.2 % of the feed particles was rejected and the diamond was recovered in the remaining 3.8 %, with an increase in grade from 0.094 % to 2.44 %.

3.4. Vertical Modes of Separation

A vertical mode of separation was considered as a neater alternative. Particles would travel by free fall in the dielectric medium, thus dispersing with vibratory transport. Field breakdown through chain contact might be reduced because chains would have less opportunity to rest on the vertical electrodes.

3.4.1. Theory

Figure 3.3 shows the generalised direction of forces for vertical dielectric separation. The angle of the particle trajectories can be found from their trigonometrical function

$$\tan \alpha = (fe - fr'')/(fg - fr') \qquad (41)$$

The resulting force is

$$f = [(fe - fr'')^2 + (fg - fr')^2]^{\frac{1}{2}} \qquad (42)$$

fe is the electrical ponderomotive force (equation 39), fg the weight of unit volume of particles in the liquid, fr'' and fr' are drag forces in the horizontal and vertical directions respectively. The direction of deflection will depend on the dielectric constant of a particle. Referring to Figure 3.2. if $\varepsilon_p - \varepsilon_\ell > 0$ particles are deflected to the left (up-gradient) and if $\varepsilon_p - \varepsilon_\ell < 0$ they are deflected to the right (down-gradient).

The real movement of the free falling particles deviates more or less from straight trajectories due to particle shape, electrical and fluid-dynamic interactions between particles and wall effects.

3.4.2. Vertical separation of arbitrary mineral mixtures

The vertical separation vessel was again built of glass plates and with the same 440 mm by 70 mm electrode as for the horizontal mode. The minimum working gap between electrodes was again 35 mm. The separator is shown in Plate 3.2. The bottom of the separator was fitted with a number of equally spaced parallel plates,

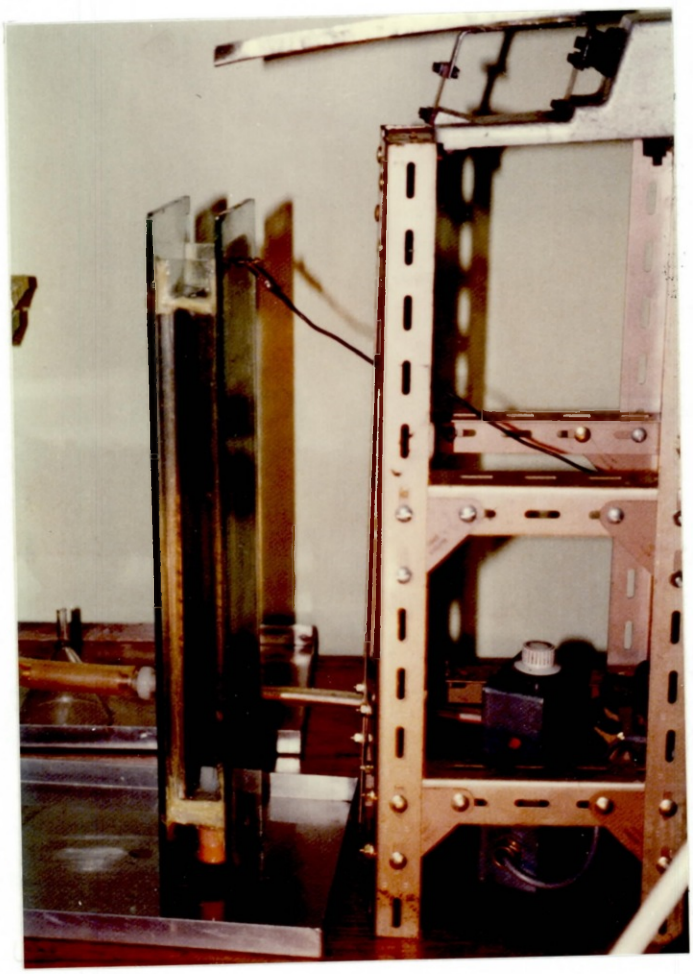

Plate 3.2. Vertical Mode of Dielectric Separation,

forming a number of slots of width 8 mm, perpendicular to the electrodes. Under the influence of the field particles were deflected from the centre line and collected in the various slots. Hence it was possible to estimate the average particle deflection.

Tests were carried out with the same ten minerals as for the horizontal separation (section 3.3.1). Table 3.4.1. shows typical results of a single pass separation at a fluid strength of 1340 kV m^{-1}. Ninety percent of the diamonds were recovered in the concentrate with 25 % of the gangue.

Table 3.4.1. shows the average deflections of the particles with the particles being fed through the separator one-by-one. The forces acting on the minerals were calculated from these deflections using the scheme of Figure 3.3. The force in N m^{-3} is given by:

$$F = (p_p - p_l)g/(H/D) \qquad (43)$$

where

p_p = particle density (kg m^{-3})

p_l = liquid density (kg m^{-3})

g = acceleration due to gravity (m sec^{-2})

H = separator height (m)

D = average deflection (m)

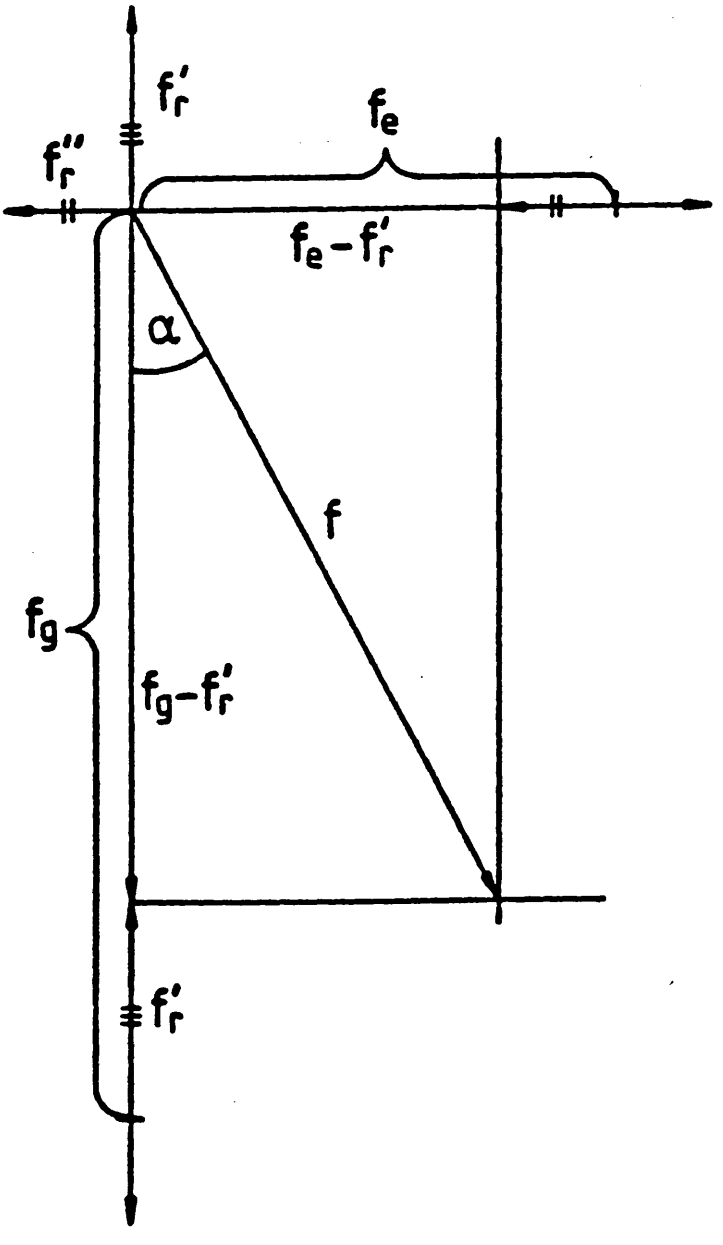

Figure 3.3. Scheme of Dielectric Deflection.

Table 3.4.1. Average deflection and force for various minerals in the concentrate.

Mineral	Average Deflection Distance mm	Force N m^{-3}	Recovery %
Diamond	-29.0	-1575	90
Quartz	- 8.6	- 306	70
White Zircon	+11.8	+ 953	30
Brown Zircon	+10.4	+ 840	30
Ilmenite	+21.0	+1719	0
Diopside	+15.6	+ 812	20
Red Garnet	+ 5.2	+ 306	40
Altered Garnet	+20.0	+1179	0
Pyrite	+23.4	+2082	30
Kimberlite	+19.9	+ 861	10
Calcite	+10.0	+ 369	20

Table 3.4.2. shows the results of treating a mixed mineral assembly of 245 particles continuously fed into the separator thus introducing the possibility of particle chaining and mechanical interactions influencing the separation. Total gangue removal rises from 63.2 % in one pass to 89.4 % in three passes, but one diamond was lost (20 %) in the second pass. Comparison with Table 3.3.1. shows that the horizontal mode gave similar results in terms of percent gangue removed (62.4 %) in one pass to 90.1 % in three) but with 100 % recovery of diamond. The difference in recovery may be insignificant in view of the small number of particles treated. Although particulate chains were formed in the vertical mode they were of insufficient length to cause field instability

Table 3.4.2. Retreatment of the concentrate in the Vertical long separator.

Mineral	Number of particles in feed	First Pass				First Retreatment				Second Retreatment			
		Concentrate		Tail		Concentrate		Tail		Concentrate		Tail	
		Number	%	Number	Total %	Number	%	Number	Total %	Number	%	Number	Total %
Diamond	5	5	100	0	0	4	80	1	20	4	80	1	20
Quartz	50	35	70	15	30	33	66	17	34	24	48	26	52
Zircon	100	50	50	50	50	26	26	74	74	17	17	83	83
Ilmenite	15	2	13.3	13	86.6	0	0	15	100	0	0	15	100
Diopside	15	2	13.3	13	86.6	0	0	15	100	0	0	15	100
Garnet (Unaltered)	15	7	46.6	8	53.3	3	20	12	80	1	6.6	14	93.3
Garnet (Altered)	15	2	13.3	13	86.6	0	0	15	100	0	0	15	100
Pyrite	15	2	13.3	13	86.6	2	13.3	13	86.6	0	0	15	100
Calcite	50	18	36	32	64	9	18	41	82	4	8	46	92
Kimberlite	15	1	6.6	14	93.2	0	0	15	100	0	0	15	100
Total	245	89		156		44		201		26		219	
% Diamond	2.04	5.6				9.1				15.4			
Total % Gangue Removed					63.8				82				89.4

and breakdown. It appeared that diamond behaviour may be less consistent in the vertical mode, hence recovery suffers. A retreatment of the tailings would lover the product grade. This is illustrated by Table 3.4.3. which gives the results of re-treatment of a tailings fraction of 142 particles containing five diamonds.

Table 3.4.3. Retreatment test on tail.

Mineral	Number in Feed	Recovery in Concentrate		Recovery from Tailing Retreat		Total Recover	
		Number	% Total	Number	% Total	Number	% Total
Diamond	5	4	80	1	20	5	100
Quartz	50	35	70	5	10	40	80
White Zircon	50	20	40	10	20	30	60
Brown Zircon	50	15	30	10	20	25	50
Ilmenite	15	3	20	3	20	6	40
Diopside	15	3	20	2	13.3	5	33.3
Red Garnet	15	3	20	3	20	6	40
Altered Garnet	15	2	13.3	2	13.3	4	26.6
Pyrite	15	3	20	3	20	6	40
Calcite	50	15	30	5	10	20	40
Kimberlite	15	0	0	0	0	0	0
Total	245	103	42.0	44	18.0	147	60.0

The retreatment of the tailings gives 100 % diamond recovery but increases the total recovery from 42 % to 60 %.

3.4.3. Comparative appraisal of vertical and horizontal operation.

1. The mass settlement of particles in the vertical mode of operation appears to cause instability of diamond trajectories.

2. The terminal velocities of particles used in these experiments (Table 3.4.4.) show Reynolds Numbers in the range of 30 - 400, corresponding to the Intermediate flow regime. Thus, non-laminar flow conditions contribute to the turbulent diversion of particles from linear trajectories.

Table 3.4.4. Typical terminal velocities of particles in the vertical separating channel.

liquid density = 1040 kg m^{-3}

liquid viscosity = 9.73 cp

Mineral	Size mm	Velocity m sec^{-1}	Re
Diamond	≈ 2.0	0.140	32
Quartz	≈ 3.5	0.125	49
Zircon	≈ 3.0	0.233	83
Ilmenite	≈ 6.0	0.350	217
Diopside	≈ 4.0	0.086	37
Garnet	≈ 4.0	0.972	413
Pyrite	≈ 4.5	0.219	109
Kimberlite	≈ 2.5	0.100	27
Calcite	≈ 3.0	0.109	39

3. The use of vibrations in the horizontal mode would tend to inhibit the mechanical entrapment of diamond

by kimberlite.

4. The horizontal mode provides a longer residence time and this may contribute to a better separation.

3.4.4. Measurement of resultant forces and comparison with calculated values.

From the average measured deflection the resultant forces on particles can be calculated by using Figure 3.3 and equation (43). Table 3.4.5. shows the resultant forces per unit volume for nine minerals, over a range of applied voltages.

Table 3.4.5. Resultant force versus applied voltage.

Mineral	Forces Nm^{-3}					
	Channel length used 300 mm			Channel length 440 mm		
	Voltage kV25	27	33	40	45	47
Diamond	+32.1	-281.0	-434.0	-450.0	-1086.0	-1575.0
Quartz	+21.0	-105.0	-152.0	-200.0	-300.0	-460.0
Zircon	+311.0	+236.0	+478.0	+590.0	+646.0	+900.0
Ilmenite	+830.2	+848.0	+1100.0	+1150.0	+1220.0	+1300.0
Diopside	+1000.0	+1249.0	+1640.0	+1700.0	+1800.0	+1900.0
Garnet	+340.0	+407.0	+900.0	+1100.0	+1250.0	+1290.0
Pyrite	+180.0	+485.0	+2620.0	+3930.0	+2000.0	+2050.0
Kimberlite	+640.2	+845.0	+1409.0	+1920.0	+1000.0	+1100.0
Calcite	+164.0	+219.0	+200.0	+436.0	+450.0	+570.0

The + and - signs show the direction of the forces.

The force increases with the applied voltage, but for diamond there is a minimum potential for deflection

between 25 and 27 kV. At this level of voltage electrical forces overcome resistive drag forces.

A comparison of calculated and measured values provides a check for the validity of equation (39).

Table 3.4.6. Calculated and measured resultant forces for diamond particles.

Voltage kV	27	33	40	45	47
r_{60^o} m	2.45×10^{-2}	2.45×10^{-2}	2.45×10^{-2}	1.9×10^{-2}	1.9×10^{-2}
Calculated force Nm^{-3}	-203.0	-304.0	-450.0	-1200.0	-1300.0
Measured force Nm^{-3}	-281.0	-434.0	-450.0	-1086.0	-1575.0

The agreement between calculated and measured values is reasonably good and thus confirms equation (39) as reasonably accurate.

3.5. Horizontal mode separator with porous membrane.

A new horizontal separator was built, capable of handling a wider range of particle sizes as well as higher throughputs and incorporating a porous membrane in order to prevent the chain induced breakdown of the applied field.

A thin membrane of strong but porous paper was inserted to prevent current conduction and field breakdown through chaining. The electrode ends were modified with copper foil to facilitate a smoother entry and exit

of particles and thus to prevent bunching of particles at those points.

The separator used the same 440 mm x 70 mm isodynamic electrode as the previous models, but the minimum gap between electrodes was 75 mm with the partition 10 mm below the upper electrode. It was established that the partition successfully protects the working space against conductive chains so that the separation remains undisturbed by field fluctuations.

Plate 3.3. shows the separation in progress with a sample of small particles (-1 mm) from the Koingmaas Mine. The applied field was 730 kV m^{-1} and the results are shown in Table 3.5.1.

Table 3.5.1. Separation of the Koingmaas sample (-1 mm)

Products	Weight	
	Grams	%
Concentrate	7.4	21.8
Tailings	26.2	78.2
Total	33.6	100.0

78 % of the feed was discarded as tailings in a single pass.

Previous tests on Kleinsee material in the old horizontal separator discarded a similar % (Table 3.3.4)

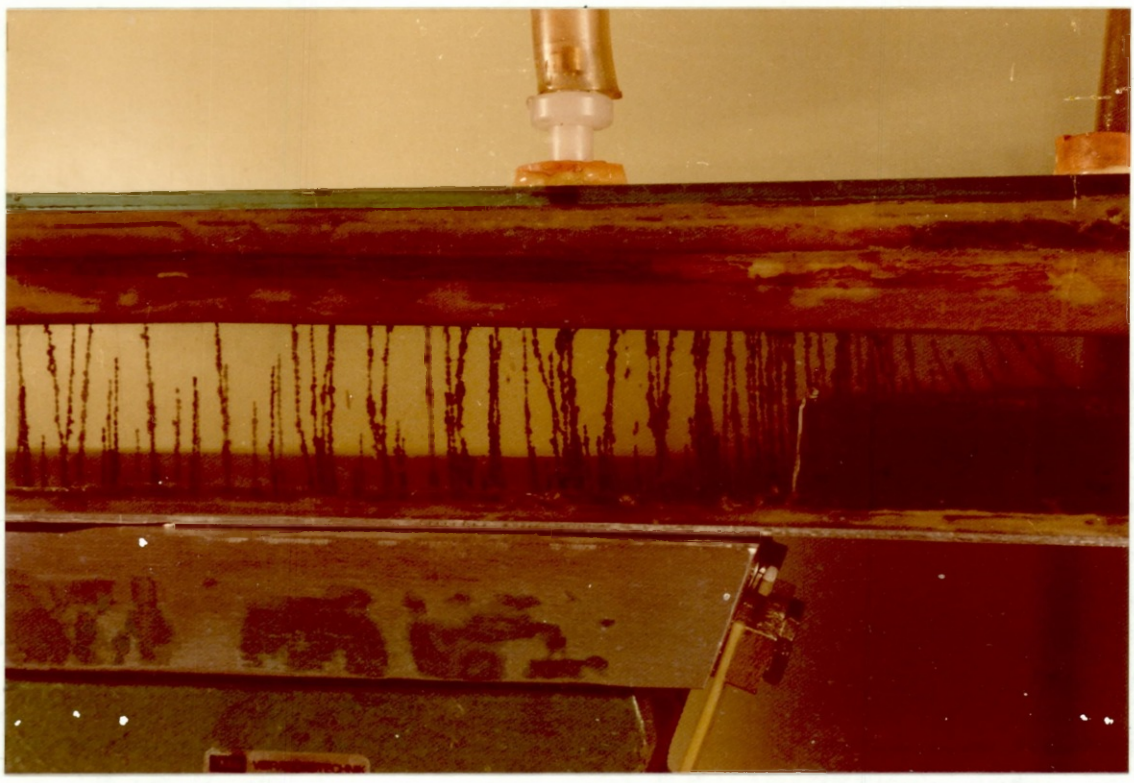

a)

b)

Plate 3.3. Separation of Koingmaas material.

but the field strength was 1270 kV m^{-1}. As the force on particles is proportional to the square of the field strength, the force required to give the same separation performance in the new channel is two thirds smaller. The separation may have been aided by the larger gap between the electrodes allowing the formation of longer chains. This results in less crowding and hence in less entrapment.

Further tests on -5 + 2 mm material were carried out with a new transformer capable of delivering voltages of up to 100 kV. Two samples of 227.5 g and 232 g respectively were provided by D.R.L. In the first sample 5 diamonds were added and 2 diamonds to the second sample. A field strength of 800 kV m^{-1} was used.

The results of the single pass separations are shown in Tables 3.5.2. (a + b).

Table 3.5.2a. Separation of a -5 + 2 mm sample with five diamonds.

Products	Weight		Diamonds	
	Grams	% Recovery	Number	% Recovery
Concentrate	27.5	12.0	5	100.0
Tailings	200.0	88.0	0	0.0
Total	227.5	100.0	5	100.0

Table 3.5.2b. Separation of a -5 + 2 mm sample containing 2 diamonds

Products	Weight		Diamonds	
	Grams	% Recovery	Number	% Recovery
Concentrate	21.7	9.0	2	100
Tailings	210.4	91.0	0	0
Total	232.1	100.0	2	100

In a further test the first concentrate was retreated. Very stable behaviour of the diamond particles were observed again. All 5 diamonds in the feed were recovered in the concentrate. The applied field was 800 kV m^{-1}.

Table 3.5.3. Concentrate retreatment tests.

Products	1st Pass		Concentrate Retretreatment		Total Recovery	
	Weight		Weight		Weight	
	Grams	% of Total	Grams	% of Total	Grams	% of Total
Concentrate	44.1	12.9	8.9	2.6	8.9	2.6
Tailings	301.0	87.1	35.2	10.3	336.2	97.4
Total	345.1	100.0	44.1	12.9	345.1	100.0

In the previous separator channel (Table 3.3.1) without a membrane, four passes were required to decrease the concentrate mass to 3.4 % of the feed whereas in this separator two passes attained 2.6 % of the feed mass with 100 % recovery of the five diamonds.

3.6. Electrode with a dual isodynamic profile.

In attempting to increase the rate of separation and hence to raise the throughput capacity of the dielctric separator, a new electrode was developed, with a profile which curves symmetrically from the longitudinal edges towards the central axis (Figure 3.4). This "double profile", electrode is 1000 mm long and 140 mm wide. Each of the two symmetrical isodynamic "wings" is 70 mm wide.

With the dual profile electrode minerals with $\varepsilon_p > \varepsilon_l$ (the majority of the minerals present) occurs laterally in opposite directions, starting from the central feed which enters at the longitudinal axis of symmetry. The diamond particles remain in the central region and should travel along the axis. If a diamond deviates on either side from the central region, the field gradient should push it back into the centre.

The dual profile electrode was tested in a vertical separating channel. In this separator the gap between electrodes is 50 mm, and the dividing area for collection of the diamond concentrate is 30 % of the total width of the electrode (Plate 3.4).

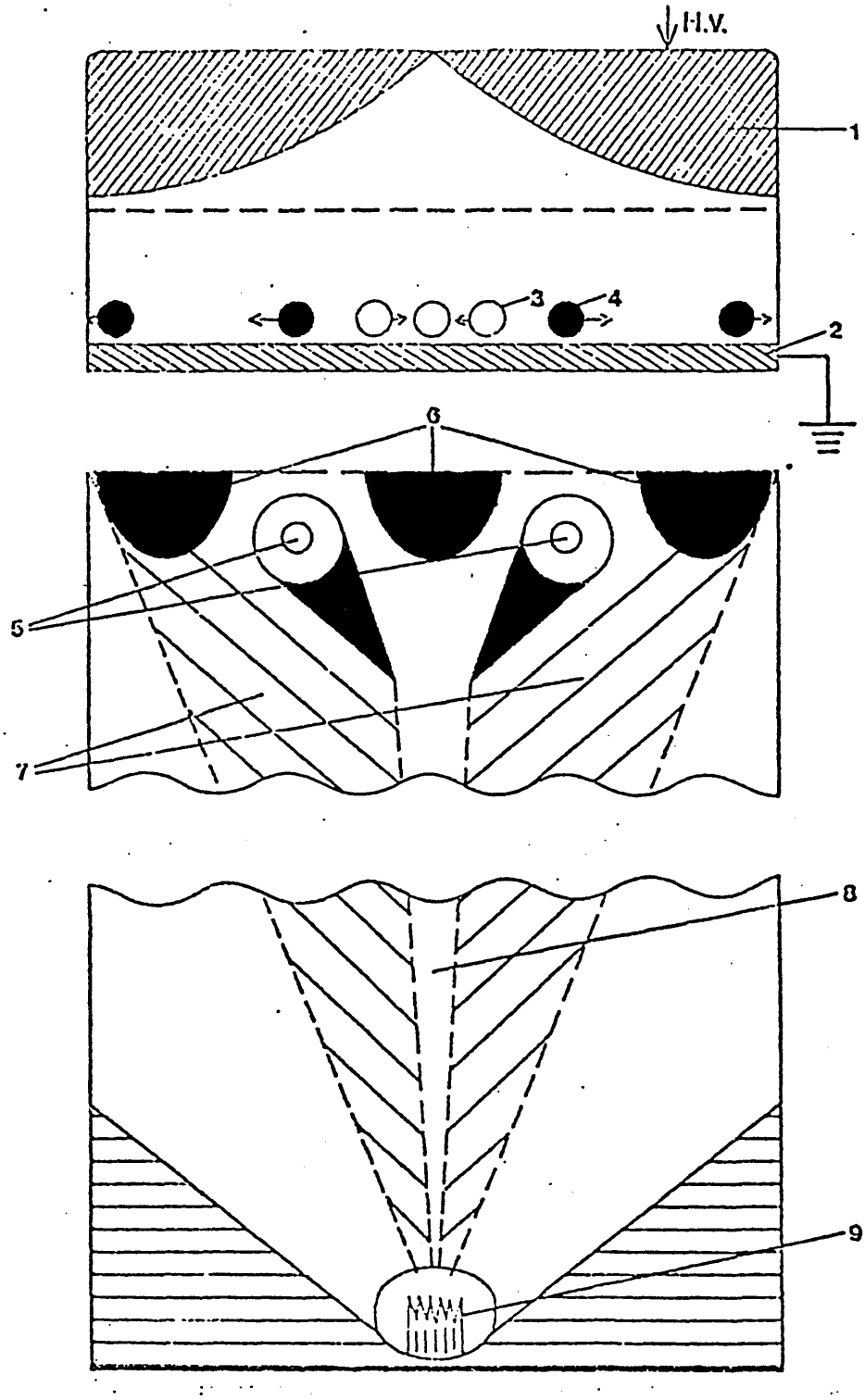

1. The High Voltage Electrode
2. The Flat Earthed Electrode
3. A Diamond Particle
4. A Kimberlite Particle
5. Adjustable Dividers
6. Discharge Orifices
7. The Kimberlite Zone
8. Zone for Diamond Recovery
9. The Feeding Point

Figure 3.4 Diagram of Double Profiled Isodynamic Dielectric Electrode

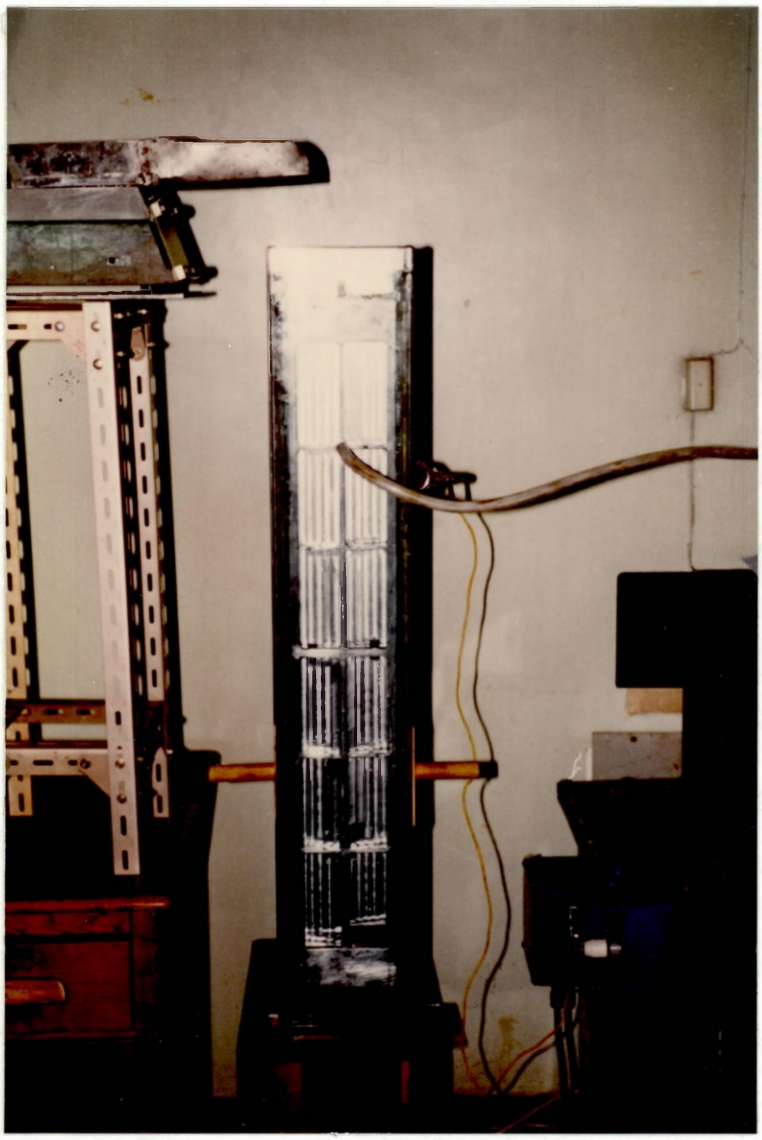

Plate 3.4. Double Profiled Electrode in Vertical Separation mode.

The results of a typical separation in the vertical mode is shown in Table 3.6.1. The Koingmass sample of 500 g was fed at a rate of 3.3 g sec^{-1}. The field strength of 1000 V m^{-1} was the maximum attainable without breakdown of the field.

Table 3.6.1. Vertical separation with double profiled electrode.

Products	Weight		Number of diamonds	
	Grams	%	Number	%
Concentrate	58.6	11.7	4	80
Tail	441.4	88.3	1	20
Total	500.0	100	5	100

This typical result shows a much higher grade of concentratethan was obtainable with the single profile electrode (Table 3.4.2) and the grade is similar to that achieved in the last horizontal channel (Tables 3.5.2a + b).

However the recovery is still not good enough, presumably due to the motional instability of the diamonds. Two possible remedies for this may be an increased applied voltage, or a larger splitter span for diamond collection.

3.7. Summary and Conclusions for the isodynamic field system

The system has been tested both in horizontal and in the vertical mode. The horizontal mode has given better results. The recovery of diamond is 100 % in a concentrate mass of about 10 % the feed in one pass. The concentrate mass was reduced to about 2 to 3 % after two passes and diamond recovery remained at 100 %. The vertical mode has proven less successful. Diamond recovery averages only 80 % and three passes are required to decrease the concentrate mass to 10 % of the feed.

An electrode with a double isodynamic profile has been tested at low voltages in the vertical mode. Although the concentrate mass was down to 10 % of the feed in one pass, the recovery of diamonds remained lower than in the horizontal mode.

REFERENCES

1. H.S. Hatfield. Dielectric Separation: A new method for the treatment of ores. Trans. Inst. Min. Metall. V233 (1924) 335-342.

H.S. Hatfield. Means and Process of Separating Substances One from Another. U.S. Patent, June 1924, No 1,498,911.

2. K.A. Nellsen and J.C. Hill. Collection of Inertialess Particles on Spheres with Electrical Force. Ind. Eng. Chem. Fundam. 15(3) (1976) 149-163.

U.S. Atomic Energy Commission. Apparatus for removing particles from a fluid. Patent No. 1,215,907 (1969).

Tobisu. Electrostatic liquid purification apparatus. U.S. Patent 4,052,289.

3. Jordan, C.E., Sullivan, G.V., Davies, B.E., Weaver, C.P. A continuous Dielectric Separator for Mineral Benefication. U.S. Bureau of Mines, R.I.8437 (1980).

Jordan, C.E., Weaver, C.P.
System for the Dielectrophoretic Separation of Particulate and Granular Material. U.S. Patent, July 1978, No 4,100,068.

4. Andres, U.Ts. Separation of Particulate Solids in Liquid Magnetics and Dielectrics. Powder Technology 26(1980) pp 83-91.

5. Electrical Methods of Diamond liberation and Separation. Imperial College Progress Report No 4. March 1981. Unpublished internal report.

Appendix One.

Calculation of kimberlite-kimberlite and kimberlite-matrix element attraction/repulsion zones.

Equation (17) is used for calculating the force between two particles

$$F = {}^{1}/_{R} \quad \frac{9(\varepsilon_l)^2 \, 4\pi\varepsilon_o \, a^3 \, (\varepsilon_p - \varepsilon_l)(\varepsilon_m - \varepsilon_l)}{(\varepsilon_p + 2\varepsilon_l)\,(\varepsilon_m + 2\varepsilon_l)^2} \cdot Eo^2 \cdot \left[1 - \sin^2\theta\cos^2\phi\left[1 + 2\,\frac{\varepsilon_m}{\varepsilon_l}\right]\right]$$

For example in an external field a kimberlite particle in the -300 + 212 μm size range may be considered in relation to a glass matrix element.

Given the following parameters

$R = 6$ mm, $a = 128$ μm $\quad \varepsilon_p = 7.4 \quad \varepsilon_m = 4.1, \quad \varepsilon_l = 6.1,$

$E^2 = [3.3 \times 10^5]^2 = 1.11 \times 10^{11}$

$$F = {}^{1}/_{6\times10^{-3}} \quad \frac{4\pi 8.84\times10^{-12}.9.(6.1)^2(1.28\times10^{-4})^3(7.4-6.1)(4.1-6.1)}{(7.4+12.2)\,(4.1+12.2)^2}$$

$$1.11 \times 10^{11} \left[1 - \sin^2\theta\cos^2\phi\left[1 + 2\,\frac{4.1}{6.1}\right]\right]$$

$$= -\,7.2 \times 10^{-10} \times [1 - \sin^2\theta\cos^2\phi\,(2.344)] \text{ Newtons}$$

$$= - \frac{7.2 \times 10^{-10}}{4/3\ \pi(1.28\times10^{-4})^3} \times [1 - \sin^2\theta\cos^2\phi(2.344)] \text{ Newtons/metre}^3$$

$$= - 81.9\ [1 - \sin^2\theta\cos^2\phi(2.344)] \text{ Newtons/metre}^3$$

Thus at the equator of the matrix element there is a repulsive force of 81.9 N m^{-3} whereas at the poles there is an attractive force of 110 N m^{-3}.

Alternatively the force between two kimberlite particles may be considered.

$R = a = 1.28 \times 10^{-4}$ m. $\varepsilon_m = \varepsilon_p = 7.4$. $E^2 = 1.11 \times 10^{11}$

$$F = \frac{1}{1.28\times10^{-4}} \frac{4\pi 8.84\times10^{-12} 9(6.1)^2 (1.28\times10^{-4})^3 (7.4-6.1)^2}{(7.4 + 12.2)^3} \cdot$$

$$\cdot 1.11 \times 10^{11} \left[1 - \sin^2\theta\cos^2\phi\left(1 + 2\ \frac{7.4}{6.1}\right)\right]$$

$$= 1.52 \times 10^{-8}\ [1 - \sin^2\theta\cos^2\phi(3.426)] \text{ Newtons}$$

$$= \frac{1.52 \times 10^{-8}}{4/3\pi(1.28\times10^{-4})^3}\ [1 - \sin^2\theta\cos^2\phi(3.426)] \text{ Newtons/metre}^3$$

$$= 1730 \times\ [1 - \sin^2\theta\cos^2\phi(3.426)] \text{ Newtons/metre}^3$$

Therefore, between two kimberlite particles there is an attractive force of 1730 N/m^3 at the equator whereas at the poles there is a repulsive force of 4193 N/m^3.

Appendix Two

Calculation of the number of kimberlite particle layers

Assumptions:

i) Only 12.5 % of the surface area of a matrix sphere is available for attracting a kimberlite particle.

ii) The kimberlite particles are spherical, having a diameter of 256 μm.

Using assumption (ii), the mass of a single kimberlite kimberlite particle can be calculated,

Kimberlite density = 2.9 g cm^{-3}

Single kimberlite particle volume = $4/3\,\pi r^3$

= $4/3 \times 3.142 \times (1.28 \times 10^{-4})^3 = 8.78 \times 10^{-12} m^3$

Thus the mass of a particle

= $2.9 \times 10^3 \times 8.78 \times 10^{-12}$ kg

= 2.54×10^{-8} kg

= 2.54×10^{-5} g

From the total weight of particles attracted the number of particles may be calculated.

The surface area of a sphere is $4\pi r^2$, with r = 0.6 cm the area is

= $4\pi(6 \times 10^{-3})^2 m^2$

= $4.5 \times 10^{-4} m^2$

With 27 spheres per layer of matrix elements, there is a total of 81 glass spheres with a surface area of 3.645×10^{-2} m^2. 12.5 % of this area is involved in kimberlite attraction = 4.56×10^{-3} m^2.

With a sphere of radius r in a square of sides 2r

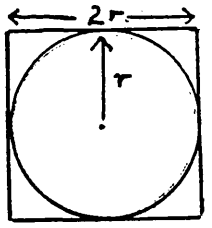

The % of space occupied by the sphere

$$= \frac{\pi r^2}{(2r)^2} = \pi/4 = 78.5\ \%$$

If the spheres are tightly packed, the area of a sphere that may be convered with kimberlite is $4.5 \times 10^{-4} \times 0.125 \times 0.785 = 4.41 \times 10^{-5} m^2$.

One kimberlite particle occupies an area of a circle of equal diameter

$$= \pi r^2 = 3.142 \times (128 \times 10^{-6})^2 m^2$$
$$= 5.15 \times 10^{-8} m^2$$

To cover a single glass sphere with a monolayer of particles

$$\frac{4.41 \times 10^{-5} m^2}{5.15 \times 10^{-3} m^2} = 856 \text{ particles}$$

To form a monolayer on 81 spheres, 69,336 particles are needed.

From the mass of one kimberlite particle, the number of deposited kimberlite particles can be calculated and also the number of particle layers formed, if the attraction is due sclely to particle matrix dipole interaction. These results are shown in Table 2.1.3.

Appendix Three.

Calculation of forces acting on kimberlite and glass particles.

The forces are calculated from equation (17)

$$F=\frac{1}{R}\ \frac{4\pi\varepsilon_o.9(\varepsilon_l)^2a^3(\varepsilon_p-\varepsilon_l)(\varepsilon_m-\varepsilon_l)[E]^2[1-\sin^2\theta\cos^2\phi[1+2\frac{\varepsilon_m}{\varepsilon_l}]]}{(\varepsilon_p+2\varepsilon_l)(\varepsilon_m+2\varepsilon_l)}$$

1) Forces between two glass particles of diameter 256 x 10^{-6} m in a field of 390 kV m^{-1}.

$R = a = 128 \times 10^{-6}$m $\quad \varepsilon_m = \varepsilon_p = 4.1 \quad \varepsilon_l = 6.1$

$E^2 = [390 \times 10^3]^2 = 1.51 \times 10^{11}$

Substituting:

$$F = \frac{1}{1.28 \times 10^{-4}} \quad \frac{4\pi 8.84\times10^{-12}.9(6.1)^2(1.28\times10^{-4})^3(4.1-6.1)^2}{(4.1+12.2)\ (4.1+12.2)^2}$$

$$\times\ 1.51 \times 10^{11}\ \left[1-\sin^2\theta\cos^2\phi(1+2\frac{4.1}{6.1})\right]$$

$= 8.5 \times 10^{-8} \times [1 - \sin^2\theta\cos^2\phi\,(2.344)]$ Newtons

$$= \frac{8.5 \times 10^{-8}}{4/3\pi(1.28\times10^{-4})^3} \times [1 - \sin^2\theta\cos^2\phi(2.344)] \text{ Newtons/metre}^3$$

$= 9676$ Newtons/metre^3

Thus, between two glass particles at the equator there is an attractive force of 9676 N/m^3. At the poles there is a repulsive force of 13,004 N/m^3.

2) Forces between a glass particle and a kimberlite particle assuming the kimberlite particle acts as the matrix element.

$R = a = 1.28 \times 10^{-4}$ m $\quad \varepsilon_m = 7.4 \quad \varepsilon_p = 6.1 \quad E^2 = 1.51 \times 10^{11}$

Thus substiting into equation (17)

$$F = \frac{1}{1.28\times10^{-4}} \frac{4\pi 8.84\times10^{-12}.9(6.1)^2(1.28\times10^{-4})^3(4.1-6.1)(7.4-6.1)}{(7.4 + 12.2)\ (4.1 + 12.2)^2}$$

$$1.51 \times 10^{11} \quad \left[1 - \sin^2\theta\cos^2\phi\left[1 + 2\,\frac{7.4}{6.1}\right]\right]$$

$$= -4.95 \times 10^{-8} \times \left[1-\sin^2\theta\cos^2\phi\left[1 + 2\,\frac{7.4}{6.1}\right]\right] \quad \text{Newtons}$$

$$= -\frac{4.59 \times 10^{-8}}{4/3\pi(1.28\times10^{-4})^3} \times \left[1 - \sin^2\theta\cos^2\phi[3.426]\right]$$

$$= -5231 \times \left[1 - \sin^2\theta\cos^2\phi[3.426]\right] \text{ Newtons/metre}^3$$

Thus between a glass particle and a kimberlite particle there is a repulsive force of 5231 N m^{-3}, whilst at the poles there is an attractive force of 12690 N m^{-3}.

3) Forces between a glass particle and a glass matrix element.

$R = 6 \times 10^{-3}$ m $\quad a = 1.28 \times 10^{-4}$m $\quad \varepsilon_m = \varepsilon_p = 4.1$

$\varepsilon_l = 6.1 \quad E^2 = 1.51 \times 10^{11}$

Substituting into (17)

$$F = \frac{1}{6\times10^{-3}} \cdot \frac{4\pi 8.84\times10^{-12} 9 (6.1)^2 (1.28\times10^{-4})^3 (4.1-6.1)(4.1-6.1)}{(4.1 + 12.2)(4.1 + 12.2)^2}$$

$$1.51 \times 10^{11} \left[1 - \sin^2\theta\cos^2\phi\left[1 + 2\frac{4.1}{6.1}\right]\right]$$

$$= 1.81 \times 10^{-9} \times [1 - \sin^2\theta\cos^2\phi\ (2.344)] \quad \text{Newtons}$$

$$= \frac{1.81 \times 10^{-9}}{4/3\pi(1.28\times10^{-4})^3} \times [1 - \sin^2\theta\cos^2\phi(2.344)] \quad \text{Newtons/metre}^3$$

$$= 207.0 \times [1 - \sin^2\theta\cos^2\phi(2.344)] \quad \text{Newtons/metre}^3$$

Thus, between a glass particle and a glass matrix element there is an equatorial attractive force of 207 N m^{-3}. At the poles there is a repulsive force of 2781 N m^{-3}.

The forces for kimberlite-kimberlite and kimberlite-glass matrix element interaction were obtained by multiplying the forces calculated in Appendix one by the ratio of the squared fields at 390 kV m^{-1} and 333.3 kV m^{-1} (by 1.36) to obtain the force value at the higher field (Table 2.1.5).